

**METASTABLE BUBBLE SOLUTIONS FOR THE ALLEN-CAHN  
EQUATION WITH MASS CONSERVATION**

*Michael J. Ward* †  
Dept. of Mathematics  
Univ. of British Columbia  
Vancouver, British Columbia  
Canada V6T 1Z2

**Abstract**

In a multi-dimensional domain, the slow motion behavior of internal layer solutions with spherical interfaces, referred to as bubble solutions, is analyzed for the nonlocal Allen-Cahn equation with mass conservation. This problem represents the simplest model for the phase separation of a binary mixture in the presence of a mass constraint. The bubble is shown to drift exponentially slowly across the domain, without change of shape, towards the closest point on the boundary of the domain. An explicit ordinary differential equation for the motion of the center of the bubble is derived by extending, to a multi-dimensional setting, the asymptotic projection method developed previously by the author to treat metastable problems in one spatial dimension. An asymptotic formula for the time of collapse of the bubble against the boundary of the domain is derived in terms of the principal radii of curvature of the boundary at the initial contact point. An analogy between slow bubble motion and the classical exit problem for diffusion in a potential well is given.

**Key Words:** Internal layers, phase separation, bubble solutions, exponentially small eigenvalues, solvability conditions, dynamic metastability.

---

† This work was supported by the NSERC grant 5-81541

## 1. Introduction

One of the simplest models for the phase separation of a binary mixture in the presence of a mass constraint is the following constrained Allen-Cahn equation introduced in [24]:

$$u_t = \epsilon^2 \Delta u + Q(u) - \sigma, \quad x \in D \subset \mathcal{R}^N, \quad (1.1a)$$

$$\partial_n u = 0, \quad x \in \partial D, \quad (1.1b)$$

$$\int_D u(x, t) dx = M. \quad (1.1c)$$

Here  $\epsilon \ll 1$ ,  $\sigma = \sigma(t)$  is a Lagrange multiplier ‘parameter’ to be determined,  $D$  is a convex domain,  $u$  is the concentration of one of the two species, and the mass  $M$  is constant. In (1.1a),  $Q(u) = -V'(u)$ , where  $V(u)$  is a double-well potential with wells of equal depth located at the two preferred phases  $s_+ > 0$  and  $s_- < 0$  where  $V(s_{\pm}) = 0$ . The non-local nature of (1.1) is reflected in the fact that  $\sigma(t)$  must satisfy  $\sigma(t) = V_0^{-1} \int_D Q[u(x, t)] dx$  in order for the mass to be conserved. Here  $V_0$  is the volume of  $D$ .

Starting from initial data, the solution to (1.1) quickly develops internal layers (or interfaces) of width  $O(\epsilon)$  that separate regions where  $u \sim s_+$  from regions where  $u \sim s_-$ . A similar phase separation process, but possibly with very complicated dynamics, leads to the formation of a pattern of internal layers for other phase transition models, including the Cahn-Hilliard equation ([10]) and the viscous Cahn-Hilliard equation ([20]). In a one-dimensional domain, some recent studies from various viewpoints (see [1], [5], [7], [11], [12], [13], [15], [17], [19], [21], [22], [23], [27]), have shown that the motion of a pattern of internal layers is exponentially slow (i. e. metastable). This metastable motion results from the exponentially weak interactions that occur between nearby layers.

The motion of internal layers in a multi-dimensional setting is usually very different than in the one-dimensional case. In a multi-dimensional domain, the interfacial motion is usually driven by the curvature of the interface and exponentially weak interactions between neighboring layers are asymptotically negligible. A notable exception to this is the work of [25] for the Allen-Cahn equation with a tri-stable  $Q(u)$  where it was shown that a steady interfacial pattern can be formed in the neck of a dumb-bell shaped region through a balance between small interfacial curvature and exponentially weak layer interactions.

For (1.1) in a multi-dimensional domain, the asymptotic analysis of [24] for  $\epsilon \rightarrow 0$  shows that the normal velocity  $v$  of a single closed interface  $\Gamma$  is given by the volume preserving mean curvature flow

$$v \sim \epsilon^2 \left( \kappa - \frac{1}{|\Gamma|} \int_{\Gamma} \kappa dS \right). \quad (1.2)$$

Here  $\kappa/2$  is the mean curvature of  $\Gamma$  and  $|\Gamma|$  denotes the area of  $\Gamma$ . It was proved in [14], and shown numerically in [9] for the case  $N = 2$ , that a closed convex interface evolving under (1.2) will tend to a spherical interface enclosing the same volume. In the case when several closed interfaces are formed from initial data, a coarsening process typically occurs, which can again ultimately lead to a single spherical interface. This process, studied in [24] for the case of non-overlapping spheres and in [8] for a collection of concentric radially symmetric interfaces, describes the growth of larger regions at the expense of smaller regions until, eventually, only a single closed interface remains.

This surviving region then tends to a spherical shape under (1.2). A natural question then is to determine the subsequent evolution of a single spherical interface contained in the domain  $D$ . Since, from (1.2),  $v = 0$  for such a spherical interface, the asymptotic analysis of [24] gives no indication on the nature of its motion.

For the related Cahn-Hilliard equation, it has been proved in [2] and [3] using a dynamical systems approach that internal layer solutions with a spherical shape, which are referred to as bubble solutions, are metastable. The main qualitative feature is that the bubble drifts exponentially slowly across the domain without changing shape, while maintaining a constant radius to conserve mass. The analysis in [2] and [3] is based on constructing an approximate invariant manifold, which captures the slow dynamics, and then proving estimates for the attractivity of this manifold. Although this analysis proves the existence of slow moving bubble solutions, further work is needed to obtain an explicit ODE that quantifies the bubble dynamics.

The goal of this paper is to give an *explicit* asymptotic characterization of a similar exponentially slow bubble motion that occurs for the analytically more tractable problem (1.1). Our analysis for (1.1) is based on an extension to a multi-dimensional setting of the asymptotic projection method developed in [27], [22] and [23] to treat metastable problems in one spatial dimension.

The outline of our analysis is as follows. In §2 the method of matched asymptotic expansions is used to construct a canonical bubble solution to the equilibrium problem for (1.1a) in all of  $\mathcal{R}^N$ . In §3 the eigenvalue problem associated with the linearization of (1.1a, b) about the canonical bubble solution is analyzed asymptotically. The analysis of this problem extends the results in [2] by providing explicit asymptotic formulas for the behavior of certain eigenfunctions on the boundary of the domain. These estimates, which are central to an explicit determination of the bubble dynamics, are derived using a boundary layer analysis. In §4 these estimates are used together with the projection method to derive an explicit ODE for the slow motion of the center  $x_0 = x_0(t)$  of a bubble. The projection method is based on linearizing (1.1) about a canonical bubble solution where the center  $x_0(t)$  is to be determined. By imposing solvability conditions for the linearized problem that must hold in the limit  $\epsilon \rightarrow 0$ , an ODE for  $x_0(t)$  is obtained. In §5 and §6 we study this ODE and determine its unstable equilibrium solution for the cases  $N = 2$  and  $N \geq 2$ , respectively. A plot of the layer structure for a bubble solution is shown in Fig. 1.

When  $N = 3$  our main asymptotic result can be summarized roughly as follows (see §6): Suppose that the bubble is inside  $D$  at  $t = 0$  and let  $x_0(0) = x_0^0 \in D \subset \mathcal{R}^N$ . Assume that at  $t = 0$  there exists a unique point  $x(\xi_0) \in \partial D$  closest to  $x_0^0$ . Then, for exponentially long times, the motion of the center of the bubble is in the direction of  $x(\xi_0) - x_0^0$ . Moreover, the distance  $r_m(t)$  between  $x(\xi_0)$  and  $x_0(t)$  satisfies the asymptotic ODE

$$\dot{r}_m \sim -\zeta r_m^{-1} \epsilon^2 (1 - r_m/R_1)^{-1/2} (1 - r_m/R_2)^{-1/2} e^{-2\nu_+^\epsilon \epsilon^{-1}(r_m - r_b)}. \quad (1.3)$$

Here  $R_1$  and  $R_2$ , with  $R_i > r_m$  for  $i = 1, 2$ , are the principal radii of curvature of  $\partial D$  at  $x(\xi_0)$  and  $r_b$  is the bubble radius. Moreover,  $\zeta$  and  $\nu_+^\epsilon$  are certain constants, which depend weakly on  $\epsilon$ , that can be calculated asymptotically for a given  $Q(u)$ .

The asymptotic analysis leading to (1.3) is valid only when the bubble is strictly contained within  $D$  (i.e.  $r_m > r_b$ ). In §7, we offer some speculations on the motion that occurs after the

bubble collapses against  $\partial D$ . In §7 we also make an analogy between the dynamics (1.3) and a similar behavior that occurs in the classical exit time problem (see [18]) for the motion of a Brownian particle confined in a domain by a potential well.

## 2. The Canonical Bubble Solution

In the limit  $\epsilon \rightarrow 0$ , we construct an equilibrium solution to (1.1a) in  $\mathcal{R}^N$  that has radial symmetry and that has exactly one internal layer centered at some  $r = r_b$ . Thus, we are to determine functions  $\sigma_b(\epsilon)$  and  $U_b(r; \epsilon)$ , called the canonical bubble solution, which satisfy

$$\epsilon^2 \Delta U_b + Q(U_b) = \sigma_b, \quad 0 < r < \infty; \quad U_b' > 0, \quad (2.1a)$$

$$U_b(r_b; \epsilon) = 0; \quad U_b(r; \epsilon) \rightarrow S_{\pm}(\epsilon), \quad \text{as } \epsilon^{-1}(r - r_b) \rightarrow \pm\infty. \quad (2.1b)$$

In (2.1a),  $Q(u)$  has exactly three zeroes on the interval  $[s_-, s_+]$  located at  $u = s_- < 0$ ,  $u = 0$ , and  $u = s_+ > 0$  with

$$Q'(s_{\pm}) < 0, \quad Q'(0) > 0, \quad V(s_+) = 0, \quad V(u) = - \int_{s_-}^u Q(\eta) d\eta. \quad (2.1c)$$

In (2.1b),  $S_{\pm}(\epsilon)$  are the asymptotic states, defined as the roots of

$$Q[S_{\pm}(\epsilon)] = \sigma_b(\epsilon), \quad (2.1d)$$

for which  $S_{\pm}(\epsilon) \rightarrow s_{\pm}$  and  $\sigma_b(\epsilon) \rightarrow 0$  as  $\epsilon \rightarrow 0$ . The internal layer location  $r_b$  is defined uniquely by  $U_b(r_b; \epsilon) = 0$ . Using the method of matched asymptotic expansions, we now construct the solution to (2.1) in three different regions: in the inner internal layer region where  $r - r_b = O(\epsilon)$  and in the two outer regions outside and inside the bubble where  $r > r_b$  and  $r < r_b$ , respectively.

### 2.1 The Internal Layer Region

In this region we introduce  $\rho = \epsilon^{-1}(r - r_b)$  and  $u_b(\rho; \epsilon) = U_b(r_b + \epsilon\rho; \epsilon)$ . Then, (2.1) becomes

$$u_b'' + \frac{\epsilon(N-1)}{r_b + \epsilon\rho} u_b' + Q(u_b) = \sigma_b, \quad -\infty < \rho < \infty, \quad (2.2a)$$

$$u_b(0; \epsilon) = 0; \quad u_b(\rho; \epsilon) \rightarrow S_{\pm}(\epsilon), \quad \text{as } \rho \rightarrow \pm\infty. \quad (2.2b)$$

To leading order as  $\epsilon \rightarrow 0$ , the solution to (2.2) is simply a planar internal layer profile. Specifically, for  $\epsilon \rightarrow 0$ , we have that  $\sigma_b(\epsilon) \rightarrow 0$ ,  $S_{\pm}(\epsilon) \rightarrow s_{\pm}$  and  $u_b(\rho; \epsilon) \rightarrow u_0(\rho)$ , where  $u_0(\rho)$  satisfies

$$u_0'' + Q(u_0) = 0, \quad -\infty < \rho < \infty; \quad u_0(0) = 0, \quad u_0'(\rho) > 0, \quad (2.3a)$$

$$u_0(\rho) \sim s_+ - a_+ e^{-\nu_+ \rho}, \quad \rho \rightarrow \infty; \quad u_0(\rho) \sim s_- + a_- e^{\nu_- \rho}, \quad \rho \rightarrow -\infty. \quad (2.3b)$$

The positive constants  $\nu_{\pm}$  and  $a_{\pm}$  in (2.3b) are defined by

$$\nu_{\pm} = \left[ -Q'(s_{\pm}) \right]^{1/2}, \quad \log a_{\pm} = \log(\pm s_{\pm}) + \int_0^{s_{\pm}} \left( \frac{\pm \nu_{\pm}}{[2V(\eta)]^{1/2}} + \frac{1}{\eta - s_{\pm}} \right) d\eta. \quad (2.3c)$$

Next, we expand the solution to (2.2) as

$$u_b(\rho; \epsilon) \sim \sum_{j=0}^{\infty} u_j(\rho) \epsilon^j, \quad \sigma_b(\epsilon) \sim \sum_{j=1}^{\infty} \sigma_j \epsilon^j. \quad (2.4a)$$

In addition, the asymptotic states  $S_{\pm}(\epsilon)$  are expanded in terms of the unknowns  $u_j(\pm\infty)$  as

$$S_{\pm}(\epsilon) \sim s_{\pm} + \sum_{j=1}^{\infty} u_j(\pm\infty)\epsilon^j. \quad (2.4b)$$

To derive an equation for  $u_j$  we substitute (2.4) into (2.2) and (2.1d). For some functions  $G_j = G_j(u_0, \dots, u_{j-1})$  and  $g_{j\pm} = g_{j\pm}(\sigma_1, \dots, \sigma_{j-1})$ , we obtain that  $u_j$ , for  $j \geq 1$ , satisfies

$$Lu_j \equiv u_j'' + Q'(u_0)u_j = \sigma_j + G_j(u_0, \dots, u_{j-1}), \quad -\infty < \rho < \infty, \quad (2.5a)$$

$$u_j(\rho) \rightarrow -\sigma_j \nu_{\pm}^{-2} + g_{j\pm}(\sigma_1, \dots, \sigma_{j-1}), \quad \text{as } \rho \rightarrow \pm\infty; \quad u_j(0) = 0. \quad (2.5b)$$

The first few functions  $G_j$  and  $g_{j\pm}$  are given explicitly by

$$G_1 = -\frac{(N-1)}{r_b} u_0', \quad G_2 = -\frac{u_1^2}{2} Q''(u_0) - \frac{(N-1)}{r_b} \left[ u_1' - \frac{\rho}{r_b} u_0' \right], \quad (2.6a)$$

$$g_{1\pm} = 0, \quad g_{2\pm} = \frac{1}{2} \sigma_1^2 \nu_{\pm}^{-6} Q''(s_{\pm}). \quad (2.6b)$$

From (2.3a) and (2.5a), it follows that  $u_0'(\rho)$  satisfies  $Lu_0' = 0$  and  $u_0'(\pm\infty) = 0$ . Therefore, the right side of (2.5a) must satisfy a solvability condition. From Green's identity and (2.3b), this condition determines  $\sigma_j$  as

$$\sigma_j = \frac{-1}{(s_+ - s_-)} \int_{-\infty}^{\infty} u_0' G_j(u_0, \dots, u_{j-1}) d\rho. \quad (2.7)$$

With  $\sigma_j$  given by (2.7), we can evaluate  $u_j(\pm\infty)$  in (2.5b). The solution to (2.5a) can then be calculated up to a multiple of  $u_0'(\rho)$ . The condition  $u_j(0) = 0$  fixes the multiple of  $u_0'$  and therefore determines  $u_j$  uniquely. Such a systematic procedure can be used to calculate all the terms  $\sigma_j$  and  $u_j$  for  $j \geq 1$ . Therefore, in principle, we can obtain full asymptotic expansions for  $u_b(\rho; \epsilon)$ ,  $\sigma_b(\epsilon)$  and  $S_{\pm}(\epsilon)$ .

The solvability condition for (2.5) with  $j = 1$  yields

$$\sigma_1 = \frac{\beta(N-1)}{(s_+ - s_-)r_b}, \quad \text{where } \beta \equiv \int_{-\infty}^{\infty} [u_0'(\rho)]^2 d\rho = \sqrt{2} \int_{s_-}^{s_+} [V(u)]^{1/2} du. \quad (2.8)$$

The function  $u_1(\rho)$  is given by

$$u_1(\rho) = \sigma_1 u_0'(\rho) \int_{-\infty}^{\rho} \frac{(u_0(\eta) - s_-)}{[u_0'(\eta)]^2} d\eta - \frac{(N-1)}{r_b} u_0'(\rho) \int_{-\infty}^{\rho} \frac{f(\eta)}{[u_0'(\eta)]^2} d\eta + D_1 u_0'(\rho). \quad (2.9)$$

Here  $f(\eta) = \int_{-\infty}^{\eta} [u_0'(z)]^2 dz$  and  $D_1$  is to be chosen so that  $u_1(0) = 0$ . In terms of  $u_0$  and  $u_1$ , the solvability condition for (2.5) with  $j = 2$  determines  $\sigma_2$  as

$$\begin{aligned} \sigma_2 = & \frac{(N-1)}{(s_+ - s_-)r_b^2} \left[ r_b \int_{-\infty}^{\infty} u_1'(\rho) u_0'(\rho) d\rho - \int_{-\infty}^{\infty} \rho [u_0'(\rho)]^2 d\rho \right] \\ & + \frac{1}{(s_+ - s_-)} \int_{-\infty}^{\infty} \frac{1}{2} [u_1(\rho)]^2 Q''[u_0(\rho)] u_0'(\rho) d\rho. \end{aligned} \quad (2.10)$$

Further coefficients are tedious to evaluate explicitly.

For some constants  $A_{j\pm}$ , it can be shown from (2.5) that  $u_b(\rho; \epsilon)$  has the far field behavior

$$u_b(\rho; \epsilon) \sim S_{\pm}(\epsilon) + \left( \sum_{j=0}^{\infty} \epsilon^j \rho^j A_{j\pm} \right) e^{\mp \nu_{\pm} \rho}, \quad \text{as } \rho \rightarrow \pm\infty. \quad (2.11)$$

Here  $A_{0\pm} = \mp a_{\pm}$  and  $A_{1\pm} = \mp(N-1)a_{\pm}/(2r_b)$ . A three-term asymptotic expansion for  $S_{\pm}(\epsilon)$  is

$$S_{\pm}(\epsilon) = s_{\pm} - \epsilon \sigma_1 \nu_{\pm}^{-2} + \epsilon^2 \left( \frac{1}{2} \sigma_1^2 \nu_{\pm}^{-6} Q''(s_{\pm}) - \sigma_2 \nu_{\pm}^{-2} \right) + O(\epsilon^3). \quad (2.12)$$

Since (2.11) is not uniformly valid for  $\rho = O(\epsilon^{-1})$ , we must construct outer solutions both inside and outside the bubble. This non-uniform behavior arises from the fact that the curvature term in (2.2a) is  $O(1)$  when  $\rho = O(\epsilon^{-1})$  and that the far field linearization of (2.2a) is done about  $s_{\pm}$  rather than  $S_{\pm}(\epsilon)$ .

## 2.2 The Outer Solutions

In the region outside the bubble for  $r > r_b$ , we write  $U_b(r; \epsilon) = S_+(\epsilon) + u_+(r; \epsilon)$ , where  $u_+ \ll S_+$ . Then, by linearizing (2.1a) about  $S_+(\epsilon)$ , we obtain that  $u_+(r; \epsilon)$  satisfies

$$u_+'' + \frac{(N-1)}{r} u_+' - (\epsilon^{-1} \nu_+^{\epsilon})^2 u_+ = 0, \quad r > r_b; \quad u_+ \rightarrow 0 \quad \text{as } r \rightarrow \infty. \quad (2.13)$$

Here  $\nu_+^{\epsilon} = \left( -Q'[S_+(\epsilon)] \right)^{1/2}$ . From (2.12) it follows that

$$\nu_+^{\epsilon} = \nu_+ \left[ 1 + \frac{\epsilon \sigma_1}{2\nu_+^4} Q''(s_+) + O(\epsilon^2) \right], \quad \text{as } \epsilon \rightarrow 0. \quad (2.14)$$

The exact solution to (2.13) is

$$u_+(r, \epsilon) = C_+ (r/r_b)^{1-N/2} K_m(\nu_+^{\epsilon} \epsilon^{-1} r), \quad m = (N-2)/2. \quad (2.15)$$

Here  $K_m(z)$ , with  $K_m(z) \sim (\pi/2z)^{1/2} e^{-z}$  as  $z \rightarrow \infty$ , is the modified Bessel function of the second kind of order  $m$ . The constant  $C_+$  in (2.15) is to be found by matching (2.15) with (2.11). To match these terms we introduce an intermediate variable  $r_{\eta}$  defined by  $r = r_b + \eta(\epsilon)r_{\eta}$ , where  $\epsilon \ll \eta(\epsilon) \ll 1$  as  $\epsilon \rightarrow 0$ . Then, in terms of  $r_{\eta}$ , (2.15) and (2.11) become to leading order

$$u_+ \sim C_+ \pi^{1/2} (2\nu_+^{\epsilon} \epsilon^{-1} r_b)^{-1/2} e^{-\nu_+^{\epsilon} \epsilon^{-1} r_b} e^{-\nu_+^{\epsilon} \epsilon^{-1} \eta(\epsilon) r_{\eta}}, \quad (2.16a)$$

$$U_b - S_+(\epsilon) \sim -a_+ e^{-\nu_+^{\epsilon} \epsilon^{-1} \eta(\epsilon) r_{\eta}}. \quad (2.16b)$$

Since  $\nu_+^{\epsilon} - \nu_+ = O(\epsilon)$ , then  $\eta(\epsilon) \epsilon^{-1} r_{\eta} (\nu_+^{\epsilon} - \nu_+) \rightarrow 0$  as  $\epsilon \rightarrow 0$ . Therefore, we can match the right sides of (2.16a) and (2.16b) to obtain

$$C_+ \sim -a_+ \pi^{-1/2} (2\nu_+^{\epsilon} \epsilon^{-1} r_b)^{1/2} e^{\nu_+^{\epsilon} \epsilon^{-1} r_b}. \quad (2.17)$$

For  $r > r_b$ , the outer solution is  $U_b(r; \epsilon) = S_+(\epsilon) + u_+(r; \epsilon)$ , where  $u_+$  is given in (2.15).

We can determine the outer solution inside the bubble, where  $0 \leq r < r_b$ , in a similar way. Substituting  $U_b(r; \epsilon) = S_-(\epsilon) + u_-(r; \epsilon)$  into (2.1a), where  $u_- \ll S_-$ , we obtain an equation for  $u_-(r; \epsilon)$ . The solution to this equation that is regular at  $r = 0$ , and which matches to (2.11) is

$$u_-(r; \epsilon) = C_- (r/r_b)^{1-N/2} I_m(\nu_-^\epsilon \epsilon^{-1} r), \quad C_- \sim a_- (2\pi\nu_-^\epsilon \epsilon^{-1} r_b)^{1/2} e^{-\nu_-^\epsilon \epsilon^{-1} r_b}. \quad (2.18)$$

Here  $I_m(z)$  is the modified Bessel function of the first kind of order  $m = (N - 2)/2$ . In (2.18), the decay constant  $\nu_-^\epsilon$  is defined by  $\nu_-^\epsilon = \left(-Q'[S_-(\epsilon)]\right)^{1/2}$ , and has the expansion

$$\nu_-^\epsilon = \nu_- \left[1 + \frac{\epsilon\sigma_1}{2\nu_-^4} Q''(s_-) + O(\epsilon^2)\right], \quad \text{as } \epsilon \rightarrow 0. \quad (2.19)$$

We summarize our results for the canonical bubble solution by using the large argument expansions of  $K_m(z)$  and  $I_m(z)$  to simplify (2.15) and (2.18). This yields,

$$U_b(r; \epsilon) \sim S_+(\epsilon) - a_+ (r/r_b)^{(1-N)/2} e^{-\nu_+^\epsilon \epsilon^{-1}(r-r_b)}, \quad r > r_b, \quad (2.20a)$$

$$U_b(r; \epsilon) = u_b(\rho; \epsilon) \sim \sum_{j=0}^{\infty} u_j(\rho) \epsilon^j, \quad \rho = \epsilon^{-1}(r - r_b) = O(1), \quad (2.20b)$$

$$U_b(r; \epsilon) \sim S_-(\epsilon) + a_- (r/r_b)^{(1-N)/2} e^{-\nu_-^\epsilon \epsilon^{-1}(r_b-r)}, \quad 0 \leq r < r_b. \quad (2.20c)$$

The functions  $u_j(\rho)$  for  $j \geq 1$  and the coefficients in the asymptotic expansions for  $S_\pm(\epsilon)$  and  $\sigma_b(\epsilon)$ , written in (2.4), can be obtained from (2.5). A few of these terms are given explicitly in (2.8), (2.9), (2.10) and (2.12).

### 2.3 Comparison of Asymptotic and Numerical Results

We now compare our asymptotic results for  $\sigma_b$  and  $\nu_\pm^\epsilon$  with corresponding numerical results computed from the full problem (2.2) using the boundary value solver COLSYS [4]. Since COLSYS allows for nonlinear boundary conditions and for interior point constraints, the problem (2.2) can be readily solved using this package by re-writing it as a first order system for the 5 unknowns  $u_b$ ,  $u'_b$ ,  $S_\pm$  and  $\sigma_b$ . We then truncate (2.2) to a finite domain  $|\rho| < L$  by imposing  $u_b(\pm L) = S_\pm$ . We chose  $L = 14$  in the computations below. To obtain numerical solutions for increasing values of  $\epsilon$ , we used a continuation strategy starting from the planar interface solution.

The computations were done for the following two forms of  $Q(u)$ :

$$Q = Q_o(u) \equiv 2(u - u^3), \quad (2.21a)$$

$$Q = Q_a(u) \equiv u(u+1)(c_0 - u)(c_1 - u); \quad c_1 = c_0 + \frac{(3 + c_0 - 2c_0^2)}{5(c_0 - 1)}, \quad c_0 = 1.2. \quad (2.21b)$$

The heteroclinic orbit constants  $\nu_\pm$ ,  $a_\pm$ ,  $s_\pm$  and  $\beta$  for  $u_0(\rho)$ , obtained from (2.3) and (2.8), are

$$Q = Q_o \implies \nu_\pm = 2, \quad a_\pm = 2, \quad s_\pm = \pm 1, \quad \beta = 4/3, \quad (2.22a)$$

$$Q = Q_a \implies \nu_+ = 1.8668, \quad \nu_- = 2.7828, \quad a_+ = 1.8000, \quad a_- = 2.2101, \\ s_+ = 1.2, \quad s_- = -1.0, \quad \beta = 1.9044. \quad (2.22b)$$

Using the values in (2.22), we can evaluate the asymptotic result for  $\nu_+^\epsilon$ , given in (2.14), and the leading order asymptotic result  $\sigma_b \sim \epsilon\sigma_1$ , where  $\sigma_1$  is given in (2.8).

When  $Q = Q_o(u)$ ,  $r_b = 1$  and  $N = 2$ , in Fig. 2 we plot the numerical solution  $u_b(\rho; \epsilon)$  to (2.2) at two values of  $\epsilon$ . For this form of  $Q(u)$  and with  $r_b = 1$ , in Fig. 3 and Fig. 4 we compare the numerically computed values of  $\nu_+^\epsilon$  and  $\sigma_b$  with the corresponding asymptotic results (2.14) and  $\sigma_b \sim \epsilon\sigma_1$ . For  $N = 2$  and  $N = 3$ , these figures show that the asymptotic results provide a close determination of the corresponding numerical results for the range  $0 < \epsilon < .15$ . In Tables 1a and 1b we show a similar agreement between the asymptotic and numerical values of  $\nu_+^\epsilon$  and  $\sigma_b$  for the form  $Q = Q_a(u)$  with  $r_b = 1$  and  $c_0 = 1.2$ .

### 3. Spectral Estimates for the Linearized Problem

We now study the spectral properties associated with linearizing the finite domain problem (1.1a, b) about the canonical bubble solution  $U_b(r; \epsilon)$ , which is defined in all of  $\mathcal{R}^N$ . The eigenvalue problem associated with this linearization is

$$\epsilon^2 \Delta \phi + Q'[U_b(r; \epsilon)]\phi = \lambda \phi, \quad x \in D, \quad (3.1a)$$

$$\partial_n \phi = 0, \quad x \in \partial D; \quad (\phi, \phi) = 1. \quad (3.1b)$$

Here  $(u, v) \equiv \int_D uv \, dx$  and  $r = |x - x_0|$ , where  $x_0$  is the location of the center of the bubble. The eigenvalues and eigenfunctions of (3.1) are labeled by  $\lambda_j$  and  $\phi_j$ , for  $j = 0, 1, \dots$ , with  $\lambda_j \rightarrow -\infty$  as  $j \rightarrow \infty$ .

In the analysis below we assume that the bubble is strictly inside  $D$  so that the distance from  $\partial D$  to the internal layer region is  $O(1)$  (see Fig. 1). With this assumption, the method of matched asymptotic expansions is used to asymptotically calculate those eigenpairs  $\lambda_j, \phi_j$  for which  $\lambda_j \rightarrow 0$  as  $\epsilon \rightarrow 0$ . The analysis is rather similar to that in §2, with the exception that we must insert a boundary layer term for  $\phi_j$  near  $\partial D$  in order to satisfy the boundary condition (3.1b) exactly. This boundary layer analysis, which gives explicit asymptotic estimates for certain  $\phi_j$  on  $\partial D$ , is valid only when  $D$  is convex. These spectral results are then used in §4.

#### 3.1 The Principal Eigenpair $\lambda_0$ and $\phi_0$

The principal eigenfunction  $\phi_0$  is radially symmetric in  $r$  except in an  $O(\epsilon)$  region near  $\partial D$ .

In the internal layer region we set  $\rho = \epsilon^{-1}(r - r_b)$  and  $\Phi_0(\rho; \epsilon) = \phi_0(r_b + \epsilon\rho)$ . Since, from (2.20b),  $U_b(r; \epsilon) \sim \sum_{j=0}^{\infty} u_j(\rho)\epsilon^j$  in this region, the coefficient  $Q'(U_b)$  in (3.1a) has the expansion

$$Q'(U_b) = Q'_0 + (\epsilon u_1 + \epsilon^2 u_2)Q''_0 + \frac{\epsilon^2}{2}u_1^2 Q'''_0 + \dots, \quad \text{as } \epsilon \rightarrow 0. \quad (3.2)$$

Here we have defined  $Q'_0 \equiv Q'(u_0)$ ,  $Q''_0 \equiv Q''(u_0)$ , etc. We then expand  $\Phi_0(\rho; \epsilon)$  and  $\lambda_0(\epsilon)$  as

$$\Phi_0(\rho; \epsilon) \sim \sum_{j=0}^{\infty} \Phi_{0j}(\rho)\epsilon^j, \quad \lambda_0(\epsilon) \sim \sum_{j=0}^{\infty} \lambda_{0j}\epsilon^j. \quad (3.3)$$

Substituting (3.2) and (3.3) into (3.1a), and collecting powers of  $\epsilon$ , we obtain, on  $-\infty < \rho < \infty$ , that

$$L\Phi_{00} = \lambda_{00}\Phi_{00}, \quad (3.4a)$$

$$L\Phi_{01} = -u_1\Phi_{00}Q_0'' - \frac{(N-1)}{r_b}\Phi_{00}' + \lambda_{01}\Phi_{00} + \lambda_{00}\Phi_{01}, \quad (3.4b)$$

$$L\Phi_{02} = -\frac{(N-1)}{r_b}\Phi_{01}' + \frac{(N-1)\rho}{r_b^2}\Phi_{00}' - u_1\Phi_{01}Q_0'' - u_2\Phi_{00}Q_0'' - \frac{1}{2}u_1^2\Phi_{00}Q_0''' \\ + \lambda_{00}\Phi_{02} + \lambda_{01}\Phi_{01} + \lambda_{02}\Phi_{00}. \quad (3.4c)$$

Here  $L$  is defined by  $Lv \equiv v'' + Q_0'v$  and we require that  $\Phi_{0i}(\rho) \rightarrow 0$  as  $\rho \rightarrow \pm\infty$ .

Since  $Lu_0' = 0$ , with  $u_0'(\pm\infty) = 0$ , the system (3.4) must satisfy the solvability condition that  $L\Phi_{0i}$ , for  $i = 0, 1, 2$ , is orthogonal to  $u_0'$  with respect to the inner product  $\langle u, v \rangle \equiv \int_{-\infty}^{\infty} uv \, d\rho$ . For (3.4a) this condition yields  $\lambda_{00} = 0$ . Thus  $\Phi_{00} = R_0u_0'$ , where  $R_0$  is a normalization constant. Substituting  $\Phi_{00} = R_0u_0'$  and  $\lambda_{00} = 0$  into (3.4b), we then re-write the right side of (3.4b) by explicitly using the equation (2.5a) (with  $j = 1$ ) satisfied by  $u_1$ . This yields

$$L\Phi_{01} = R_0Lu_1' + \lambda_{01}R_0u_0'. \quad (3.5)$$

Since  $\langle Lu_1', u_0' \rangle = \langle u_1', Lu_0' \rangle = 0$ , the solvability condition for (3.5) gives  $\lambda_{01} = 0$ . Therefore,  $\Phi_{01} = R_0u_1'$ . The arbitrary multiple of  $u_0'$ , which can be added to  $\Phi_{01}$ , can be chosen to be zero. Substituting  $\Phi_{0i} = R_0u_i'$  and  $\lambda_{0i} = 0$  for  $i = 1, 2$  into (3.4c), and using (2.5a) with  $j = 2$ , we can re-write (3.4c) as

$$L\Phi_{02} = R_0 \left( Lu_2' - \frac{(N-1)}{r_b^2}u_0' \right) + \lambda_{02}R_0u_0'. \quad (3.6)$$

The solvability condition for (3.6) gives  $\lambda_{02} = (N-1)r_b^{-2}$  and, thus,  $\Phi_{02} = R_0u_2'$ . Therefore, the inner expansion for  $\phi_0$  is

$$\Phi_0(\rho; \epsilon) = R_0 \left[ u_0'(\rho) + \epsilon u_1'(\rho) + \epsilon^2 u_2'(\rho) + O(\epsilon^3) \right], \quad (3.7)$$

and the expansion of the eigenvalue is

$$\lambda_0(\epsilon) = \epsilon^2 \frac{(N-1)}{r_b^2} + O(\epsilon^3). \quad (3.8)$$

Although  $\lambda_0$  is positive, and hence would normally lead to exponential growth, this mode is suppressed in §4 by the presence of the mass constraint.

In the outer region for  $r < r_b$  we let  $\phi_0 \sim R_0\phi_-(r; \epsilon)$ . In this region  $U_b \sim S_-(\epsilon)$ , so that (3.1a) becomes

$$\phi_-'' + \frac{(N-1)}{r}\phi_-' - (\epsilon^{-1}\tilde{\nu}_-^\epsilon)^2\phi_- = 0, \quad 0 < r < r_b; \quad \tilde{\nu}_-^\epsilon = \nu_-^\epsilon [1 + \lambda_0/(\nu_-^\epsilon)^2]^{1/2}. \quad (3.9)$$

Since  $\lambda_0 = O(\epsilon^2)$  as  $\epsilon \rightarrow 0$ , it follows that  $\nu_-^\epsilon - \tilde{\nu}_-^\epsilon = O(\epsilon^2)$ . The exact solution to (3.9), which is regular at  $r = 0$ , and which matches to (3.7) is

$$\phi_-(r; \epsilon) = B_-(r/r_b)^{1-N/2} I_m(\tilde{\nu}_-^\epsilon \epsilon^{-1}r), \quad B_- \sim a_- \nu_- (2\pi \nu_-^\epsilon \epsilon^{-1}r_b)^{1/2} e^{-\tilde{\nu}_-^\epsilon \epsilon^{-1}r_b}, \quad (3.10)$$

where  $m = (N-2)/2$ .

In the outer region for  $r > r_b$ , but at an  $O(1)$  distance away from  $\partial D$ , we write  $\phi_0 \sim R_0 \phi_+(r; \epsilon)$ . In this region  $U_b \sim S_+(\epsilon)$ , so that (3.1a) becomes

$$\phi_+'' + \frac{(N-1)}{r} \phi_+' - (\epsilon^{-1} \tilde{\nu}_+^\epsilon)^2 \phi_+ = 0, \quad r > r_b; \quad \tilde{\nu}_+^\epsilon = \nu_+^\epsilon [1 + \lambda_0/(\nu_+^\epsilon)^2]^{1/2}. \quad (3.11)$$

Note that  $\tilde{\nu}_+^\epsilon - \nu_+^\epsilon = O(\epsilon^2)$ . The exact solution to (3.11), which matches to (3.7), is

$$\phi_+(r; \epsilon) = B_+ (r/r_b)^{1-N/2} K_m(\tilde{\nu}_+^\epsilon \epsilon^{-1} r), \quad B_+ \sim a_+ \nu_+ \pi^{-1/2} (2\nu_+^\epsilon \epsilon^{-1} r_b)^{1/2} e^{\tilde{\nu}_+^\epsilon \epsilon^{-1} r_b}, \quad (3.12)$$

where  $m = (N-2)/2$ .

Notice that  $\phi_+$  is exponentially small for  $r > r_b$ , and has the following asymptotic estimate on  $\partial D$ :

$$\partial_n \phi_+ = \tilde{\nu}_+^\epsilon \epsilon^{-1} B_+ (r/r_b)^{1-N/2} K_m'(\tilde{\nu}_+^\epsilon \epsilon^{-1} r) [\hat{r} \cdot \hat{n} + O(\epsilon)], \quad \text{where } r = |x - x_0|, \quad x \in \partial D. \quad (3.13)$$

Here  $\hat{n}$  is the unit outward normal to  $\partial D$ ,  $\hat{r} = (x - x_0)r^{-1}$  and  $\hat{r} \cdot \hat{n}$  denotes the dot product. The analysis leading to (3.13) requires that  $D$  is convex.

In §4 we need an asymptotic formula for  $\phi_0$  on  $\partial D$ . However, since  $\phi_+$  fails to exactly satisfy the boundary condition (3.1b), we cannot use  $\phi_+$  directly to obtain this formula. Instead, to estimate  $\phi_0$  on  $\partial D$ , we must first add a boundary layer term to  $\phi_+$  which is localized near  $\partial D$ . To represent  $\phi_0$  near  $\partial D$ , we introduce a local coordinate system defined near  $\partial D$ . We set  $\eta = n/\epsilon$ , where  $-n$  is the distance from  $x \in D$  to  $\partial D$ , and we let  $\xi$  denote  $N-1$  coordinates orthogonal to  $n$ . In the region  $\eta = O(1)$ , we write  $\phi_0 = R_0(\phi_+ + \phi_L)$ , where  $\phi_L = \phi_L(\eta, \xi)$  is the boundary layer function. Then, to leading order, we obtain from (3.1) that

$$\begin{aligned} \partial_{\eta\eta} \phi_L - (\tilde{\nu}_+^\epsilon)^2 \phi_L &= 0, \quad \eta < 0; \quad \phi_L \rightarrow 0, \quad \text{as } \eta \rightarrow -\infty, \\ \partial_\eta \phi_L &= \epsilon h(\xi), \quad \eta = 0; \quad h(\xi) \equiv -[\partial_n \phi_+] \Big|_{\eta=0}. \end{aligned} \quad (3.14)$$

The solution to (3.14), which decays exponentially as  $\eta \rightarrow -\infty$ , is

$$\phi_L = (\epsilon h(\xi)/\tilde{\nu}_+^\epsilon) e^{\tilde{\nu}_+^\epsilon \eta}. \quad (3.15)$$

From (3.13), (3.15) and  $\phi_0 = R_0(\phi_+ + \phi_L)$ , we obtain in an  $O(\epsilon)$  neighborhood of  $\partial D$  that

$$\phi_0 \sim R_0 B_+ (r/r_b)^{1-N/2} \left[ K_m(\tilde{\nu}_+^\epsilon \epsilon^{-1} r) - e^{\tilde{\nu}_+^\epsilon n \epsilon^{-1}} \left( \hat{r} \cdot \hat{n} K_m'(\tilde{\nu}_+^\epsilon \epsilon^{-1} r) \right) \Big|_{\eta=0} \right]. \quad (3.16)$$

Finally, using (3.12), the result  $\tilde{\nu}_+^\epsilon = \nu_+^\epsilon + O(\epsilon^2)$ , and the large argument asymptotics of  $K_m$  and  $K_m'$ , we calculate on  $\partial D$  that

$$\phi_0 \sim R_0 a_+ \nu_+ (r/r_b)^{(1-N)/2} e^{-\nu_+^\epsilon \epsilon^{-1} (r-r_b)} [1 + \hat{r} \cdot \hat{n}], \quad r = |x - x_0|, \quad x \in \partial D. \quad (3.17)$$

We can summarize our results for  $\phi_0$  by using  $\tilde{\nu}_\pm^\epsilon \sim \nu_\pm^\epsilon$  and the large argument expansions of  $K_m(z)$ ,  $I_m(z)$  and  $K_m'(z)$  to simplify (3.10) and (3.12). This yields

$$\phi_0 \sim R_0 a_- \nu_- (r/r_b)^{(1-N)/2} e^{-\nu_-^\epsilon \epsilon^{-1} (r_b-r)}, \quad 0 \leq r < r_b, \quad (3.18a)$$

$$\phi_0 \sim R_0 \left[ u_0'(\rho) + \epsilon u_1'(\rho) + \epsilon^2 u_2'(\rho) + \dots \right], \quad \rho = \epsilon^{-1} (r - r_b) = O(1), \quad (3.18b)$$

$$\phi_0 \sim R_0 a_+ \nu_+ (r/r_b)^{(1-N)/2} e^{-\nu_+^\epsilon \epsilon^{-1} (r-r_b)}, \quad r > r_b, \quad n = O(1). \quad (3.18c)$$

To normalize  $\phi_0$  by  $(\phi_0, \phi_0) = 1$ , we note that  $R_0^{-1}\phi_0$  is  $O(1)$  for  $r - r_b = O(\epsilon)$ , but is exponentially small elsewhere. Therefore, a Laplace-type evaluation of this inner product yields

$$(\phi_0, \phi_0) \sim \epsilon R_0^2 \Omega_N r_b^{N-1} \int_{-\infty}^{\infty} [u_0(\rho)']^2 d\rho, \quad \implies \quad R_0 \sim (\Omega_N \epsilon r_b^{N-1} \beta)^{-1/2}. \quad (3.19)$$

Here  $\Omega_N$  is the surface area of the unit ball in  $\mathcal{R}^N$  and  $\beta$  is defined in (2.8). A similar asymptotic evaluation provided

$$(\phi_0, 1) \sim \epsilon R_0 \Omega_N r_b^{N-1} (s_+ - s_-) = O(\epsilon^{1/2}). \quad (3.20)$$

Finally, since  $\phi_0$  has no nodal lines it is clear that  $\phi_0$  must be the first eigenfunction. The principal eigenvalue  $\lambda_0(\epsilon)$  has the estimate (3.8).

### 3.2 The Translation Eigenfunctions

Let  $U_b(r; \epsilon)$  satisfy (2.1) with  $r = |x - x_0|$ , and let  $x_j$  and  $x_{0j}$  denote the  $j^{\text{th}}$  coordinate of  $x$  and  $x_0$ , respectively. Then, by differentiating (2.1a) with respect to  $x_j$ , we obtain for  $j = 1, \dots, N$  that

$$\epsilon^2 \Delta [\partial_{x_j} U_b(r; \epsilon)] + Q'(U_b) [\partial_{x_j} U_b(r; \epsilon)] = 0. \quad (3.21)$$

By comparing (3.21) and (3.1a), it is clear that the eigenvalue problem (3.1a) in  $\mathcal{R}^N$  has  $N$  zero eigenvalues with eigenfunctions  $\phi_j = \partial_{x_j} U_b(r; \epsilon)$  for  $j = 1, \dots, N$ . In  $\mathcal{R}^N$ , these zero eigenvalues are a consequence of the translation invariance. For the finite domain problem, the bubble is assumed to be strictly inside  $D$ , and thus it follows from (2.20a) that  $\partial_{x_j} U_b(r; \epsilon)$  fails to satisfy the boundary condition (3.1b) by only exponentially small terms. Therefore, it is natural to expect that the translation eigenvalues and eigenfunctions associated with the infinite domain problem get perturbed only very slightly by the presence of the finite domain. Specifically, we show that (3.1) has  $N$  exponentially small eigenvalues  $\lambda_j$  with corresponding eigenfunctions  $\phi_j \sim R_j [\partial_{x_j} U_b + \phi_{Lj}]$ , for  $j = 1, \dots, N$ . Here,  $R_j$  is a normalization constant and  $\phi_{Lj}$  is a boundary layer function localized near  $\partial D$ , which allows (3.1b) to be satisfied. To estimate  $\lambda_j$ , we can use Green's identity applied to (3.1a) and  $\partial_{x_j} U_b$  to derive

$$\lambda_j (\partial_{x_j} U_b, \phi_j) = -\epsilon^2 \int_{\partial D} \phi_j \partial_n [\partial_{x_j} U_b] dS, \quad (3.22)$$

where  $dS$  is the surface area element on  $\partial D$ . Substituting  $\phi_j \sim R_j [\partial_{x_j} U_b + \phi_{Lj}]$  and (2.20a) into (3.22) we find, for  $j = 1, \dots, N$ , that  $\lambda_j = O(\epsilon^p e^{-C\epsilon^{-1}})$  for some  $p$  and  $C > 0$ . A more precise estimate for  $\lambda_j$  is given below once we have determined  $\phi_{Lj}$ .

To calculate  $\phi_{Lj}$  we set  $U_b \sim S_+(\epsilon)$  and  $\lambda = 0$  in (3.1a). Then, near  $\partial D$ , we write (3.1) in terms of the local  $(\eta, \xi)$  coordinate system introduced in §3.1. To leading order,  $\phi_{Lj}$  satisfies

$$\begin{aligned} \partial_{\eta\eta} \phi_{Lj} - (\nu_+^\epsilon)^2 \phi_{Lj} &= 0, \quad \eta < 0; & \phi_{Lj} &\rightarrow 0, \quad \text{as } \eta \rightarrow -\infty, \\ \partial_\eta \phi_{Lj} &= \epsilon h(\xi), \quad \eta = 0; & h(\xi) &\equiv -\partial_n [\partial_{x_j} U_b] \Big|_{\eta=0}. \end{aligned} \quad (3.23)$$

By solving (3.23) we obtain  $\phi_{Lj}$  and thus

$$\phi_j = R_j \left[ \partial_{x_j} U_b + (\epsilon h(\xi) / \nu_+^\epsilon) e^{\nu_+^\epsilon \eta} \right], \quad (3.24)$$

where  $-n$  is the distance from  $x \in D$  to  $\partial D$ .

In §4 we require an asymptotic formula for  $\phi_j$  on  $\partial D$ . To derive such a formula, we use (2.20a) to obtain on  $\partial D$  that

$$\partial_{x_j} U_b = \nu_+^\epsilon a_+ r^{-1} \epsilon^{-1} (r/r_b)^{(1-N)/2} e^{-\nu_+^\epsilon \epsilon^{-1}(r-r_b)} [(x_j - x_{0j}) + O(\epsilon)], \quad (3.25a)$$

$$\partial_n [\partial_{x_j} U_b] = -(\nu_+^\epsilon)^2 a_+ r^{-1} \epsilon^{-2} (r/r_b)^{(1-N)/2} e^{-\nu_+^\epsilon \epsilon^{-1}(r-r_b)} (x_j - x_{0j}) [\hat{r} \cdot \hat{n} + O(\epsilon)]. \quad (3.25b)$$

Therefore, by substituting (3.25) and (2.20a) into (3.24) and by replacing  $\nu_+^\epsilon$  by  $\nu_+$  in the pre-exponential factors, we obtain the following asymptotic formula for  $\phi_j$  on  $\partial D$  for  $j = 1, \dots, N$ :

$$\phi_j \sim R_j \nu_+ a_+ \epsilon^{-1} r^{-1} (r/r_b)^{(1-N)/2} e^{-\nu_+^\epsilon \epsilon^{-1}(r-r_b)} (x_j - x_{0j}) [1 + \hat{r} \cdot \hat{n}], \quad x \in \partial D. \quad (3.26)$$

In (3.25) and (3.26),  $r = |x - x_0|$ ,  $\hat{r} = (x - x_0)r^{-1}$ , and  $\hat{n}$  is the unit outward normal to  $\partial D$ .

To estimate  $\lambda_j$  and  $R_j$  we need to evaluate  $(\partial_{x_j} U_b, \partial_{x_j} U_b)$  for  $\epsilon \rightarrow 0$ . From (2.20) it follows that the dominant contribution to this integral arises from the region near  $r = r_b$ . Therefore, using (2.20b) for  $U_b$ , we calculate that

$$(\partial_{x_j} U_b, \partial_{x_j} U_b) \sim (\epsilon N)^{-1} r_b^{N-1} \beta \Omega_N. \quad (3.27)$$

Here  $\beta$  is defined in (2.8) and  $\Omega_N$  is the surface area of the unit ball in  $\mathcal{R}^N$ . Therefore, for  $\epsilon \rightarrow 0$ , the normalization constant  $R_j$  satisfies

$$R_j \sim [\epsilon N / (r_b^{N-1} \beta \Omega_N)]^{1/2}. \quad (3.28)$$

Next, by substituting (3.25b), (3.26), (3.27) and  $\phi_j \sim R_j \partial_{x_j} U_b$  into (3.22), we obtain the following asymptotic formula for the exponentially small eigenvalues  $\lambda_j$  for  $j = 1, \dots, N$ :

$$\lambda_j \sim \frac{a_+^2 \nu_+^3 N}{\beta \Omega_N} \int_{\partial D} r^{1-N} e^{-2\nu_+^\epsilon \epsilon^{-1}(r-r_b)} \left( \frac{x_j - x_{0j}}{r} \right)^2 \hat{r} \cdot \hat{n} [1 + \hat{r} \cdot \hat{n}] dS. \quad (3.29)$$

In §5 and §6 we use Laplace's method to asymptotically evaluate the surface integral in (3.29). However, from (3.29), it is immediately clear that, for some  $p$ ,  $\lambda_j = O(\epsilon^p e^{-2\nu_+^\epsilon \epsilon^{-1}(r_{max} - r_b)})$ . Here  $r_{max}$  is the radius of the largest ball in  $\mathcal{R}^N$ , centered at  $x_0$ , that can be inscribed within  $D$ .

Finally, in §4, we need a rough asymptotic estimate for the inner product  $(\phi_j, 1)$ . Since, by symmetry, the integral of  $\phi_j$  vanishes identically on radially symmetric domains centered at  $x_0$ , it follows from the exponential decay of  $\phi_j$  for  $r > r_b$  that

$$(\phi_j, 1) = O\left(\epsilon^p e^{-\nu_+^\epsilon \epsilon^{-1}(r_{max} - r_b)}\right), \quad \text{for } j = 1, \dots, N. \quad (3.30)$$

### 3.3 The Other Eigenpairs with $\lambda_j \rightarrow 0$ as $\epsilon \rightarrow 0$

For simplicity we consider only the two-dimensional case  $N = 2$ . In §3.1 and §3.2 we calculated  $\phi_j$  and  $\lambda_j$  for  $j = 0, 1, 2$ . We now calculate the other eigenpairs for which  $\lambda_j \rightarrow 0$  as  $\epsilon \rightarrow 0$ . Since these other eigenvalues are negative and since mass is conserved we are lead to the conclusion that

the radially symmetric bubble solution is stable with respect to infinitesimal perturbations having zero mean.

In the internal layer region, these eigenfunctions for  $m = 2, 3, \dots$  have the following form

$$\phi_{2m-1} = \Phi_m[\epsilon^{-1}(r - r_b); \epsilon] \cos(m\theta), \quad \phi_{2m} = \Phi_m[\epsilon^{-1}(r - r_b); \epsilon] \sin(m\theta). \quad (3.31)$$

Here  $(r, \theta)$  is a polar coordinate system centered at  $x_0$ . The corresponding eigenvalues  $\lambda_{2m-1}(\epsilon)$  and  $\lambda_{2m}(\epsilon)$  can each be expanded in powers of  $\epsilon$ . The coefficients in these expansions, which are determined from the internal layer region, are found to agree to all orders in  $\epsilon$ . Therefore, to within all algebraic terms in  $\epsilon$ , we have  $\lambda_{2m-1}(\epsilon) \sim \lambda_m^*(\epsilon)$  and  $\lambda_{2m}(\epsilon) \sim \lambda_m^*(\epsilon)$ . For an arbitrary domain that is not concentric with  $r = r_b$ , we expect that the gap width  $\lambda_{2m}(\epsilon) - \lambda_{2m-1}(\epsilon)$  is exponentially small as  $\epsilon \rightarrow 0$ . However, we do not estimate the gap width here.

Substituting  $\lambda = \lambda_m^*$  and (3.31) into (3.1a), we obtain on  $-\infty < \rho < \infty$ , that  $\Phi_m(\rho; \epsilon)$  satisfies

$$\Phi_m'' + \frac{\epsilon}{r_b + \epsilon\rho} \Phi_m' - \frac{\epsilon^2 m^2}{(r_b + \epsilon\rho)^2} \Phi_m + Q'(U_b) \Phi_m = \lambda_m^* \Phi_m, \quad \Phi_m(\pm\infty) = 0. \quad (3.32)$$

Here  $\rho = \epsilon^{-1}(r - r_b)$ . Next, we expand  $\lambda_m^*(\epsilon)$  and  $\Phi_m(\rho; \epsilon)$  as

$$\Phi_m(\rho; \epsilon) \sim \sum_{j=0}^{\infty} \Phi_{mj}(\rho) \epsilon^j, \quad \lambda_m^*(\epsilon) \sim \sum_{j=0}^{\infty} \lambda_{mj}^* \epsilon^j. \quad (3.33)$$

Substituting (3.2) and (3.33) into (3.32), and collecting powers of  $\epsilon$ , we obtain that  $\Phi_{mj}(\rho)$ , for  $j \geq 0$ , satisfies a system similar to (3.4). The system for  $\Phi_{mj}$  for  $j = 0, 1, 2$  is obtained by setting  $N = 2$  in (3.4), replacing  $\Phi_{0j}$  and  $\lambda_{0j}$  in (3.4) by  $\Phi_{mj}$  and  $\lambda_{mj}^*$ , and adding the new term  $m^2 r_b^{-2} \Phi_{m0}$  to the right side of (3.4c). Therefore, by repeating the calculations in (3.5) – (3.8), we readily obtain for  $m = 2, 3, \dots$  that

$$\Phi_m(\rho; \epsilon) \sim R_m \left[ u_0'(\rho) + \epsilon u_1'(\rho) + \epsilon^2 u_2'(\rho) + O(\epsilon^3) \right], \quad (3.34a)$$

$$\lambda_{2m}(\epsilon) \sim \lambda_{2m-1}(\epsilon) \sim \lambda_m^*(\epsilon) = \epsilon^2 \frac{(1 - m^2)}{r_b^2} + O(\epsilon^3). \quad (3.34b)$$

The eigenfunctions are then given by combining (3.34a) and (3.31). The normalization constant  $R_m$ , chosen so that  $(\phi_{2m}, \phi_{2m}) = 1$ , is given asymptotically by

$$R_m \sim (\epsilon \pi r_b \beta)^{-1/2}. \quad (3.35)$$

In a similar way as was done in §3.1, we can calculate the behavior of the eigenfunctions  $\phi_{2m-1}$  and  $\phi_{2m}$  in the two outer regions inside and outside the bubble. Since the results from such an analysis are not needed later we do not carry out the details here. In §4 we only need an order of magnitude estimate for the inner products  $(\phi_{2m}, 1)$  and  $(\phi_{2m-1}, 1)$ . This estimate can be obtained from the observations that these inner products vanish identically on radially symmetric domains centered at  $x_0$ , and the eigenfunctions are exponentially small in the outer regions where  $r > r_b$ . Therefore, the estimate (3.30) also holds for these inner products. Such an estimate also holds

for any eigenfunction  $\phi_j$  of (3.1) in  $\mathcal{R}^N$ , with  $N \geq 2$ , that is not radially symmetric but that is localized near  $r = r_b$  and is exponentially small for  $r > r_b$ .

### 3.4 Comparison of Asymptotic and Numerical Results

For each of the two forms of  $Q(u)$  given in (2.21) we use COLSYS ([4]) to numerically compute the principal eigenvalue  $\lambda_0$  as a function of  $\epsilon$ . When  $Q = Q_o$  and  $r_b = 1$ , in Fig. 5 we compare, for  $N = 2$  and  $N = 3$ , the numerically computed  $\lambda_0$  with the asymptotic result (3.8). This figure shows the close agreement between the asymptotic and numerical results for  $\lambda_0$  over the range  $0 < \epsilon < .20$ . For the case  $Q = Q_a$ ,  $r_b = 1$  and  $c_0 = 1.2$  in (2.21b), in Table 2a we show the favorable agreement between the asymptotic and numerical values for  $\lambda_0$  over the same range in  $\epsilon$ .

For the form  $Q = Q_o$  with  $r_b = 1$  and  $N = 2$ , in Table 2b we compare the asymptotic formula (3.34b) for  $\lambda_3$  and  $\lambda_4$  with corresponding full numerical results computed from (3.32) using COLSYS. The asymptotic results for these higher eigenvalues are again found to be in close agreement with the numerical results.

### 4. The Analysis of Slow Bubble Dynamics using the Projection Method

We now consider the time-dependent problem (1.1) for  $u = u(x, t)$  and  $\sigma = \sigma(t)$ , where the mass  $M$  in (1.1c) is constant. We assume that the initial data for (1.1) is a canonical bubble solution  $u(x, 0) = U_b[|x - x_0^0|; \epsilon]$  with  $\sigma = \sigma_b(\epsilon)$ . Alternatively, we can view this initial data as representing the end result of a coarsening process that has taken place between many bubbles. The bubble is assumed to lie entirely within  $D$  and, as shown in Appendix A, its radius  $r_b$  can be calculated for  $\epsilon \rightarrow 0$  in terms of the mass  $M$  as

$$r_b = r_b^0 + \epsilon r_b^1 + O(\epsilon^2), \quad \text{where} \quad r_b^0 = \left[ \left( \frac{N}{\Omega_N} \right) \left( \frac{V s_+ - M}{s_+ - s_-} \right) \right]^{1/N}. \quad (4.1)$$

Here  $V$  is the volume of  $D$  and the correction term  $r_b^1$  is given explicitly in (A.5a).

We now look for a solution to (1.1) where the bubble is translated without change of shape. The projection method is used to determine the trajectory  $x_0 = x_0(t)$ , with  $x_0(0) = x_0^0$ , of the center of the bubble. The analysis below is valid up until the edge of the bubble is at an  $O(\epsilon)$  distance from  $\partial D$ .

To use the projection method we first set  $u(x; t) = U_b[|x - x_0|; \epsilon] + w(x, t)$  and  $\sigma(t) = \sigma_b + \mu(t)$ , where  $x_0 = x_0(t)$ . Assuming that  $w \ll U_b$  and  $\mu \ll \sigma_b$  uniformly in time, we obtain the following linearized problem from (1.1):

$$L_\epsilon w \equiv \epsilon^2 \Delta w + Q'(U_b)w = \partial_t U_b + \mu + w_t, \quad x \in D, \quad (4.2a)$$

$$\partial_n w = -\partial_n U_b, \quad x \in \partial D, \quad (4.2b)$$

$$\int_D w dx = 0; \quad w(x, 0) = 0. \quad (4.2c)$$

We then expand  $w = \sum_{j=0}^{\infty} c_j(t) \phi_j$ , where  $\phi_j$  for  $j \geq 0$  are the normalized eigenfunctions of (3.1). Since  $r = |x - x_0(t)|$  in (3.1a), these eigenfunctions now depend parametrically on time. Applying Green's identity to (3.1) and (4.2a, b) we derive

$$(w_t, \phi_j) - (w, L_\epsilon \phi_j) = -\epsilon^2 \int_{\partial D} \phi_j \partial_n U_b dS - (\partial_t U_b, \phi_j) - \mu(1, \phi_j), \quad (4.3)$$

where  $(u, v) \equiv \int_D uv \, dx$ . Now since  $c_j(t) = (\phi_j, w)$  and  $(\phi_j, \phi_j) = 1$ , we calculate that

$$c_j' - (\phi_j, w_t) = (w, \phi_{jt}) = \sum_{k=0}^{\infty} c_k (\phi_k, \phi_{jt}) = \sum_{\substack{k=0 \\ k \neq j}}^{\infty} c_k (\phi_k, \phi_{jt}). \quad (4.4)$$

Next, substituting  $L_\epsilon \phi_j = \lambda_j \phi_j$  and (4.4) into (4.3), we find that  $c_j(t)$  for  $j = 0, 1, \dots$ , satisfies

$$c_j' - \lambda_j c_j - \sum_{\substack{k=0 \\ k \neq j}}^{\infty} c_k (\phi_k, \phi_{jt}) = F_j; \quad c_j(0) = 0. \quad (4.5a)$$

Here  $F_j$  is defined by

$$F_j = -(\partial_t U_b, \phi_j) - \mu(1, \phi_j) - B_j. \quad (4.5b)$$

In (4.5a),  $\lambda_j$  is an eigenvalue of (3.1) and we have defined the boundary term  $B_j$  by

$$B_j = \epsilon^2 \int_{\partial D} \phi_j \partial_n U_b \, dS. \quad (4.6)$$

Using (2.20a) to calculate  $\partial_n U_b$ , we find

$$B_j \sim \epsilon a_+ \nu_+^\epsilon \int_{\partial D} \phi_j (r/r_b)^{(1-N)/2} e^{-\nu_+^\epsilon \epsilon^{-1}(r-r_b)} \hat{r} \cdot \hat{n} \, dS. \quad (4.7)$$

In addition, to satisfy the mass constraint in (4.2c) we require that

$$\sum_{j=0}^{\infty} c_j(\phi_j, 1) = 0. \quad (4.8)$$

Using the asymptotic estimates for  $\phi_j$  and  $\lambda_j$  obtained in §3, we now derive  $N+1$  consistency conditions that determine the function  $\mu = \mu(t)$  and an evolution equation for the  $N$ -vector  $x_0(t)$ . These conditions are that (4.8) is asymptotically satisfied and that each  $c_j(t)$  in (4.5a) is exponentially small over the exponentially long time interval induced by the exponentially small eigenvalues  $\lambda_j$  for  $j = 1, \dots, N$ . These two conditions are sufficient to ensure that  $w \ll U_b$  uniformly in time. It is easy to show from (3.1) that  $(\phi_k, \phi_{jt}) = -(\phi_j, \phi_{kt})$  and that  $(\phi_k, \phi_{jt})$  is exponentially small. Thus, the last term on the left side of (4.5a) corresponds to a skew-symmetric matrix. Since such a matrix does not lead to exponential growth of  $c_j(t)$  in (4.5a), this term is insignificant in the derivation of the consistency conditions below.

When the bubble is strictly inside  $D$ , we recall from §3 that  $\lambda_0 > 0$  with  $\lambda_0 = O(\epsilon^2)$ , that  $\lambda_1, \dots, \lambda_N$  are exponentially small and that  $\lambda_j < 0$  with  $\lambda_j = O(\epsilon^2)$  for  $j \geq N+1$ . Thus, in (4.5a), the only terms that can lead to growth in  $c_j(t)$  are those corresponding  $j = 0, 1, \dots, N$ . In addition, by comparing (3.20) with (3.30) it follows that  $(\phi_j, 1)$  for  $j \geq 1$  is exponentially smaller than  $(\phi_0, 1)$ . Therefore, to asymptotically satisfy the constraint (4.8) we require that  $c_0(t) = 0$  for all time. Thus, to eliminate exponential growth for  $c_0(t)$  on the time interval  $t = O(\lambda_0^{-1})$ , we require that the right side of (4.5a) vanish when  $j = 0$ . Next, we observe from (3.26), (3.28) (3.29) and (4.7) that, although  $B_j$  is exponentially small, it has the same exponential estimate as that for the

exponentially small eigenvalues. Therefore, unless the right side of (4.5a) vanishes for  $j = 1, \dots, N$ , we would obtain an  $O(1)$  response for  $c_j(t)$  over the exponentially long time intervals induced by  $\lambda_1, \dots, \lambda_N$ . This would then violate the assumption that  $w \ll U_b$ . Therefore, we must require that the right side of (4.5a) vanish for  $j = 1, \dots, N$ . In summary, the  $N + 1$  consistency conditions are that

$$(\partial_t U_b, \phi_j) = -\mu(1, \phi_j) - B_j, \quad j = 0, \dots, N. \quad (4.9)$$

Finally, notice that when  $j \geq N + 1$ , the right side of (4.5a) is exponentially small and  $\lambda_j = O(\epsilon^2)$  with  $\lambda_j < 0$ . Since  $c_j(t)$  for  $j \geq N + 1$  is decreasing in time, the conditions (4.9) are sufficient to ensure that  $w$  is exponentially small uniformly in time.

There are three main observations, which follows from the results in §3, that enable us to asymptotically decouple (4.9) into two separate sub-systems: one for  $j = 0$  and the other for  $j = 1, \dots, N$ . Firstly, from (3.17), (3.19), (3.26) and (3.28), we observe that  $B_j$  in (4.7) has the *same* asymptotic order as  $\epsilon \rightarrow 0$  for each  $j = 0, \dots, N$ . Secondly, it follows from (3.20) and (3.30) that  $(\phi_0, 1)$  is exponentially *larger* than  $(\phi_j, 1)$  for  $j = 1, \dots, N$ . Thirdly, if we choose the time scale so that  $(\partial_t U_b, \phi_j)$  for  $j = 1, \dots, N$  has the same asymptotic order as  $B_j$  for  $j = 1, \dots, N$ , then since  $\phi_0$  is radially symmetric (except in a  $O(\epsilon)$  region near  $\partial D$ ), it follows that  $(\partial_t U_b, \phi_0)$  is exponentially *smaller* than  $B_0$ . These three observations show that we can neglect the left side of (4.9) when  $j = 0$  and we can neglect the term  $(1, \phi_j)$  for  $j = 1, \dots, N$ . Therefore, using (4.7), we obtain the following asymptotically decoupled problem for  $x_0(t)$  and  $\mu(t)$ :

$$\mu(1, \phi_0) \sim -\epsilon a_+ \nu_+^\epsilon \int_{\partial D} \phi_0(r/r_b)^{(1-N)/2} e^{-\nu_+^\epsilon \epsilon^{-1}(r-r_b)} \hat{r} \cdot \hat{n} dS, \quad (4.10a)$$

$$(\partial_t U_b, \phi_j) \sim -\epsilon a_+ \nu_+^\epsilon \int_{\partial D} \phi_j(r/r_b)^{(1-N)/2} e^{-\nu_+^\epsilon \epsilon^{-1}(r-r_b)} \hat{r} \cdot \hat{n} dS, \quad j = 1, \dots, N. \quad (4.10b)$$

Next, we evaluate the various terms in (4.10). To evaluate  $\phi_j$  on  $\partial D$ , we use the estimate (3.17) for  $j = 0$  and the estimate (3.26) for  $j = 1, \dots, N$ . The inner product  $(\phi_0, 1)$  is estimated in (3.20). Finally, to calculate  $(\partial_t U_b, \phi_j)$  for  $j = 1, \dots, N$  we note that the dominant contribution to this integral arises from the region near  $r = r_b$ . Substituting  $\partial_t U_b = -U_b' \hat{r} \cdot \dot{x}_0$  and  $\phi_j \sim R_j \partial_{x_j} U_b$  into this inner product, we obtain, for  $j = 1, \dots, N$ , that

$$(\partial_t U_b, \phi_j) \sim -R_j \dot{x}_{0j} \int_{\mathcal{R}^N} [U_b']^2 r^{-2} (x_j - x_{0j})^2 dx = -\frac{R_j}{N} \dot{x}_{0j} \int_{\mathcal{R}^N} [U_b'(r; \epsilon)]^2 r^{N-1} dr d\Omega_N. \quad (4.11)$$

Here  $\dot{x}_{0j} \equiv dx_{0j}/dt$ . Then, using (2.20b), (4.11) becomes

$$(\partial_t U_b, \phi_j) \sim -R_j \dot{x}_{0j} (\epsilon N)^{-1} \Omega_N r_b^{N-1} \beta, \quad j = 1, \dots, N. \quad (4.12)$$

By substituting (3.17), (3.26), (3.20) and (4.12) into (4.10) we obtain the following slow motion result:

**Proposition (Slow Motion Result):** *Assume that the bubble solution for (1.1) is strictly inside of  $D$  and that  $D$  is convex. Then, the slow motion of the bubble is described by  $u(x; t) \sim U_b[|x - x_0(t)|; \epsilon]$  and  $\sigma \sim \sigma_b + \mu(t)$ , where*

$$\mu(t) \sim -\frac{a_+^2 \nu_+^2}{\Omega_N (s_+ - s_-)} \int_{\partial D} r^{1-N} e^{-2\nu_+^\epsilon \epsilon^{-1}(r-r_b)} [1 + \hat{r} \cdot \hat{n}] \hat{r} \cdot \hat{n} dS, \quad (4.13a)$$

$$\dot{x}_0 \sim \frac{\epsilon N a_+^2 \nu_+^2}{\Omega_N \beta} \int_{\partial D} r^{1-N} e^{-2\nu_+^\epsilon \epsilon^{-1}(r-r_b)} \hat{r} [1 + \hat{r} \cdot \hat{n}] \hat{r} \cdot \hat{n} dS. \quad (4.13b)$$

In (4.13),  $r = r(\xi, t) \equiv |x(\xi) - x_0(t)|$ ,  $\hat{r} = \hat{r}(\xi, t) \equiv [x(\xi) - x_0(t)]/r(\xi)$ ,  $\hat{n} = \hat{n}(\xi)$  is the unit outward normal to  $\partial D$ ,  $\Omega_N$  is the surface area of the unit  $N$ -ball, and  $\xi = (\xi_1, \dots, \xi_{N-1})$  are the surface coordinates that parametrize  $\partial D$ . In addition,  $r_b$ ,  $a_+$ ,  $\nu_+$  and  $\nu_+^\epsilon$  are given in (4.1), (2.3c), (2.3c) and (2.14), respectively. The following result for the equilibrium problem is an immediate consequence of (4.13):

**Corollary (Equilibrium Bubble Location):** *When  $D$  is convex, the equilibrium location  $x_0 = x_0^\epsilon$  for the center of the bubble satisfies*

$$\int_{\partial D} r^{-N} e^{-2\nu_+^\epsilon \epsilon^{-1}(r-r_b)} (x_j - x_{0j}) [1 + \hat{r} \cdot \hat{n}] \hat{r} \cdot \hat{n} dS = 0, \quad j = 1, \dots, N. \quad (4.14)$$

The equilibrium value of  $\mu$  is obtained by setting  $x_0 = x_0^\epsilon$  in (4.13a).

The geometrical implications of (4.13) and (4.14) for the dynamics and the equilibria of the bubble solution are examined in §5 for the case  $N = 2$  and in §6 for the case  $N \geq 2$ .

### 5. Slow Bubble Motion in $N = 2$ Dimensions

We now examine the dynamics under (4.13b) when  $N = 2$ . In this case  $\xi$  is arclength along  $\partial D$  and thus  $dS = d\xi$  in (4.13). Suppose that at time  $t = 0$ , the distance  $r(\xi, 0) = |x(\xi) - x_0(0)|$  is minimized at a unique point  $x(\xi_0) \in \partial D$  with arclength coordinate  $\xi = \xi_0$ . In the limit  $\epsilon \rightarrow 0$ , we now show from (4.13b) that  $x(\xi_0)$  remains the closest point on  $\partial D$  to  $x_0(t)$  as  $t$  increases.

To show this we need to introduce some notation. Let  $\xi = \xi_m(t)$ , with  $\xi_m(0) = \xi_0$ , denote the arclength coordinate at time  $t$  where the minimum value of  $r(\xi, t) = |x(\xi) - x_0(t)|$  over all  $x(\xi) \in \partial D$  is attained. Assume that  $\xi_m(t)$  is the unique such minimum point. We want to show that  $\dot{\xi}_m = 0$ . Let  $r_m = r_m(t) \equiv r[\xi_m(t), t]$  denote the minimum distance from  $x_0(t)$  to  $\partial D$  at time  $t$  and let  $\hat{r}_m(t)$  denote the unit vector  $\hat{r}_m(t) = (x[\xi_m(t)] - x_0(t)) r_m^{-1}$ . For  $\xi_m(t)$  to be the minimizer, the following necessary condition must hold

$$x'[\xi_m(t)] \cdot \hat{r}_m(t) = 0. \quad (5.1)$$

Now, for  $\epsilon \rightarrow 0$ , the dominant contribution to the integral in (4.13b) arises from the region  $\xi \approx \xi_m(t)$  where  $r(\xi, t)$  is minimized. Since  $\xi$  is arclength, the Taylor expansion of  $r(\xi, t)$  near  $\xi_m(t)$  is

$$r(\xi, t) = r_m + \frac{1}{2} (r_m^{-1} + \kappa_m) (\xi - \xi_m)^2 + \dots, \quad \text{as } \xi \rightarrow \xi_m. \quad (5.2)$$

Here  $\kappa_m$  is the curvature of  $\partial D$  at  $\xi = \xi_m(t)$ . Since  $D$  is assumed to be convex, then  $\kappa_m \leq 0$ . Next, using (5.2) and the condition  $\hat{r}_m \cdot \hat{n} = 1$  that holds at the minimum point, we can use Laplace's method on (4.13b) to obtain

$$\dot{x}_0 \sim \epsilon^{3/2} \zeta \frac{r_m^{-1/2}}{(1 + \kappa_m r_m)^{1/2}} e^{-2\nu_+^\epsilon \epsilon^{-1}(r_m - r_b)} \hat{r}_m, \quad \text{as } \epsilon \rightarrow 0. \quad (5.3a)$$

Here we have defined  $\zeta$  by

$$\zeta = 2a_+^2 \nu_+^2 \beta^{-1} (\pi \nu_+^\epsilon)^{-1/2}. \quad (5.3b)$$

In deriving (5.3a) we have assumed that the strict inequality  $\kappa_m r_m > -1$  holds so that  $r_{\xi\xi} > 0$  at  $\xi_m(t)$ .

Since, from (5.3a),  $\dot{x}_0$  is in the direction of  $\hat{r}_m(t)$ , it follows that  $\dot{r}_m(t) < 0$ . Since this distance is decreasing, the surface coordinate where  $r(\xi, t)$  is minimized cannot be a discontinuous function of  $t$ . Therefore, we can assume that  $\xi = \xi_m(t)$  is differentiable. Finally, to establish that  $\dot{\xi}_m = 0$ , we first differentiate (5.1) with respect to  $t$  to get

$$\dot{\xi}_m (1 + \kappa_m r_m) = x'(\xi_m) \cdot \dot{x}_0. \quad (5.4)$$

Then, from (5.1), (5.3a) and (5.4), it is clear that  $\dot{\xi}_m = 0$ . Hence,  $\xi_m(t) = \xi_0$  for  $t > 0$ . Finally, we can use Laplace's method on (4.13a) to calculate  $\mu(t)$ . We summarize our result as follows:

**Proposition (Slow Bubble Motion for  $N = 2$ ):** *Assume that at  $t = 0$ ,  $x(\xi_0)$  is the unique point on  $\partial D$  which is closest to  $x_0(0) = x_0^0$ . Then, for  $\epsilon \rightarrow 0$ , the motion of the center of the bubble is in the direction of  $x(\xi_0) - x_0^0$  for exponentially long times, and the distance  $r_m(t) = |x(\xi_0) - x_0(t)|$  satisfies the asymptotic ODE*

$$\dot{r}_m \sim -\frac{\epsilon^{3/2} \zeta r_m^{-1/2}}{(1 + \kappa_m r_m)^{1/2}} e^{-2\nu_+^\epsilon \epsilon^{-1}(r_m - r_b)}. \quad (5.5)$$

In addition,  $\mu(t)$  satisfies

$$\mu \sim -\frac{\zeta \beta \epsilon^{1/2}}{2(s_+ - s_-)} \frac{r_m^{-1/2}}{(1 + \kappa_m r_m)^{1/2}} e^{-2\nu_+^\epsilon \epsilon^{-1}(r_m - r_b)}. \quad (5.6)$$

Here  $\kappa_m$  is the curvature of  $\partial D$  at  $\xi_0$  and  $\zeta$  is defined in (5.3b).

Using Laplace's method on (3.29), we can also calculate the exponentially small eigenvalues  $\lambda_j$  for  $j = 1, 2$ . We find that

$$\lambda_j \sim \frac{\zeta \epsilon^{1/2} \nu_+ r_m^{-1/2}}{(1 + \kappa_m r_m)^{1/2}} \left[ \hat{r}_m \cdot \hat{i}_j \right]^2 e^{-2\nu_+^\epsilon \epsilon^{-1}(r_m - r_b)}, \quad j = 1, 2. \quad (5.7)$$

Here  $\hat{i}_j$  is the unit basis vector in the  $x_j^{\text{th}}$  direction.

The dynamics (5.5) is asymptotically valid provided that  $r_m(t) > r_b$ . When  $r_m(t) - r_b = O(\epsilon)$ , the bubble begins to collapse against  $\partial D$  on a faster time-scale. We define an approximate collapse time  $t_c$  by the condition  $r_m(t_c) = r_b$ . Suppose that  $r_m(0) = r_0 > r_b$ . From (5.5),  $t_c$  is given by

$$t_c = \frac{\epsilon^{-3/2}}{\zeta} \int_{r_b}^{r_0} z^{1/2} (1 + \kappa_m z)^{1/2} e^{2\nu_+^\epsilon \epsilon^{-1}(z - r_b)} dz. \quad (5.8)$$

We can then integrate (5.8) by parts twice to obtain, for  $\epsilon \rightarrow 0$ , that

$$t_c \sim \frac{\epsilon^{-1/2}}{2\zeta \nu_+^\epsilon} f(r_0) \left[ 1 - \frac{\epsilon}{4\nu_+^\epsilon} \left( \frac{1}{r_0} + \frac{\kappa_m}{1 + \kappa_m r_0} \right) \right] e^{2\nu_+^\epsilon \epsilon^{-1}(r_0 - r_b)}. \quad (5.9)$$

Here  $f(r_0) \equiv r_0^{1/2} (1 + \kappa_m r_0)^{1/2}$ . To evaluate the exponentiated terms in (5.5) and (5.9) we use the two term expansions for  $\nu_+^\epsilon$  and  $r_b$  given in (2.14) and (A.4). These terms are significantly more accurate than if evaluated them by using only the leading order behaviors  $\nu_+^\epsilon \sim \nu_+$  and  $r_b \sim r_b^0$ .

### 5.1 Explicit Examples of Slow Dynamics

To generate convex domains we follow [16]. Let the origin be contained in  $D$  and let  $(x_1, x_2)$  be a point on  $\partial D$ . Let  $p$  denote the perpendicular distance from the origin to the tangent line to  $\partial D$  that passes through  $(x_1, x_2)$ . Let  $\theta$  denote the angle between this perpendicular line and the positive  $x_1$  axis. Then, when  $\theta$  ranges over  $0 \leq \theta \leq 2\pi$ , we sweep out a closed domain  $D$  whose boundary is given parametrically by

$$x_1(\theta) = p(\theta) \cos(\theta) - p'(\theta) \sin(\theta), \quad x_2(\theta) = p(\theta) \sin(\theta) + p'(\theta) \cos(\theta). \quad (5.10)$$

The curvature  $\kappa(\theta)$  of  $\partial D$ , the length  $L$  of  $\partial D$ , and the area  $V$  of  $D$  are given in terms of  $p(\theta)$  by

$$\kappa(\theta) = - \left[ p(\theta) + p''(\theta) \right]^{-1}, \quad L = \int_0^{2\pi} p(\theta) d\theta, \quad V = \frac{1}{2} \int_0^{2\pi} \left( [p(\theta)]^2 - [p'(\theta)]^2 \right) d\theta. \quad (5.11)$$

Thus given any  $p(\theta)$  with  $p(\theta) = p(\theta + 2\pi)$ ,  $p(\theta) > 0$  and  $p(\theta) + p''(\theta) > 0$ , we obtain the boundary of a strictly convex domain ( $\kappa < 0$ ).

We now illustrate our results for two choices of  $p(\theta)$  and for the two choices of  $Q(u)$  given in (2.21) (see (2.22) for some heteroclinic orbit constants for these  $Q(u)$ ). For convenience, in the examples below we give the radius  $r_b$  and then calculate the mass  $M = M(\epsilon)$  in terms of  $r_b$  using (A.2). To calculate  $M$  and the terms in (5.5) for each choice of  $Q(u)$ ,  $r_b$  and  $\epsilon$ , we need to evaluate  $\sigma_1$ ,  $\nu_+^\epsilon$ ,  $\zeta$  and  $\theta_\pm$  given in (2.8), (2.14), (5.3b) and (A.3), respectively. When  $Q = Q_o(u)$ ,  $r_b = .75$  and  $\epsilon = .15$ , we use (2.21a) and (2.22a) to obtain

$$\sigma_1 = 8/9, \quad \nu_+^\epsilon = 1.9, \quad \theta_\pm = \log 2, \quad \zeta = 9.8233. \quad (5.12a)$$

Alternatively, when  $Q = Q_a(u)$ ,  $r_b = .75$  and  $\epsilon = .15$ , we find from (2.21b) and (2.22b) that

$$\sigma_1 = 1.1542, \quad \nu_+^\epsilon = 1.8176, \quad \theta_+ = 0.7980, \quad \theta_- = 0.5173, \quad \zeta = 4.9625. \quad (5.12b)$$

In the examples below, solutions to (5.5) were computed using the Sandia ODE solver [26]. The dynamical re-scaling method of [27] was used to generate appropriate time steps.

**Example 5.1:** Let  $p(\theta) = 3 + 0.4 \sin^3(\theta) - 0.5 \cos^2(\theta)$ ,  $Q = Q_o(u)$ ,  $r_b = .75$  and  $\epsilon = .15$ . From (5.11) we obtain that  $V = 23.34$  and from (5.12a), (2.22a) and (A.2) we calculate that  $M = 19.03$ . In Fig. 6 we show the motion of the center of the bubble starting from the three different initial conditions labeled by  $O_i$ , for  $i = 1, 2, 3$ . The closest point on  $\partial D$  to  $O_i$  (labeled by  $\star$  in Fig. 6) is computed numerically and the curvature  $\kappa_m$  of  $\partial D$  at this closest point, which is needed in (5.5), is calculated from (5.11). The bubble then moves in the direction of the arrows and begins to collapse against  $\partial D$  when its center is at  $C_i$ . In Fig. 7 we plot the function  $\log_{10}(1 + t)$  versus  $r_m - r_b$  for each of the three initial conditions. Notice that the bubble is essentially stationary over a very long time interval. For each  $i$ , in Table 3 we give the coordinates of the initial location  $O_i$  and we give the initial distance  $r_m(0)$  to  $\partial D$ . We also show the favorable comparison between the asymptotic collapse time (5.9) and the corresponding numerical value computed from (5.5).

**Example 5.2:** Let  $p(\theta) = 3 + 1.4 \sin^3(\theta)$ ,  $Q = Q_a(u)$ ,  $r_b = .75$  and  $\epsilon = .15$ . From (5.11), (5.12b), (2.22b) and (A.2) we calculate that  $V = 26.74$  and  $M = 26.72$ . In Fig. 8 we plot the motion

of the center of the bubble for three different initial conditions. The corresponding trajectories  $\log_{10}(1+t)$  versus  $r_m - r_b$  are shown in Fig. 9. The coordinates of the initial conditions and a comparison of the asymptotic and numerical values for the collapse times are given in Table 4.

## 5.2 The Equilibrium Bubble Location $N = 2$

For  $\epsilon \rightarrow 0$ , we now use (4.14) to determine the center  $x_0 = x_0^\epsilon$  of the (unstable) equilibrium bubble solution. Suppose that the center  $x_{in}$  of the largest inscribed circle  $\mathcal{B}$  for  $D$  is uniquely defined. In particular, this occurs when  $D$  is strictly convex (i.e.  $\kappa < 0$  on  $\partial D$ ). In this case, we show that  $x_0^\epsilon$  is located at an  $O(\epsilon)$  distance from  $x_{in}$ . In other words,  $x_0^\epsilon$  is asymptotically close to that point in  $D$  which is furthest from the boundary.

Suppose that  $\mathcal{B}$  is uniquely determined and that  $\mathcal{B}$  is tangent to  $\partial D$  at exactly two points  $x(\xi_1) \in \partial D$  and  $x(\xi_2) \in \partial D$  with  $\xi_1 \neq \xi_2$ . Let  $r_{in}$  be the radius of  $\mathcal{B}$  and let  $\mathcal{C}$  be the chord joining  $x(\xi_1)$  and  $x(\xi_2)$ . We assume that the order of contact of  $\mathcal{B}$  with  $\partial D$  is such that the strict inequality  $\kappa_i r_{in} > -1$  holds for  $i = 1, 2$ . Here  $\kappa_i$  is the curvature of  $\partial D$  at  $\xi = \xi_i$ . Let  $\hat{n}_i$  be the unit outward normal to  $\partial D$  at  $\xi_i$ . Then, the following local conditions must hold at  $\xi_1$  and  $\xi_2$ :

$$\hat{n}_1 = -\hat{n}_2; \quad \frac{(x(\xi_i) - x_{in})}{|x(\xi_i) - x_{in}|} \cdot \hat{n}_i = 1, \quad i = 1, 2. \quad (5.13a)$$

Moreover, since  $\mathcal{B}$  makes exactly two-point contact with  $\partial D$ , the following global condition must be satisfied:

$$|x(\xi) - x_{in}| - r_{in} > 0, \quad \forall x(\xi) \in \partial D, \quad \text{with } \xi \neq \xi_1, \xi \neq \xi_2. \quad (5.13b)$$

From (5.13b) it is clear that if we set  $x_0^\epsilon = x_{in}$  in (4.14), the dominant contribution to the integral in (4.14) would arise from the regions near  $\xi_1$  and  $\xi_2$ . Therefore, by using Laplace's method on (4.14) together with (5.13a), we find that (4.14) is asymptotically satisfied when  $\kappa_1 = \kappa_2$ . Thus, in this case, the center of the equilibrium bubble solution coincides with the center  $x_{in}$  of  $\mathcal{B}$ . An example of this case is illustrated in Fig. 10 where we show the location of the equilibrium bubble solution corresponding to the domain given in Fig. 6.

When the curvatures at the two contact points are unequal, the bubble center  $x_0^\epsilon$  still lies on  $\mathcal{C}$  but is now at an  $O(\epsilon)$  distance from  $x_{in}$ . Let  $r_i = |x(\xi_i) - x_0^\epsilon|$  and  $\hat{r}_i = (x(\xi_i) - x_0^\epsilon)r_i^{-1}$  for  $i = 1, 2$ . Since  $x_0^\epsilon \in \mathcal{C}$  and  $|x_0^\epsilon - x_{in}| = O(\epsilon)$ , we have  $\hat{r}_i \cdot \hat{n}_i = 1$ ,  $\hat{r}_1 = -\hat{r}_2$  and  $r_1 - r_2 = O(\epsilon)$ . These relations are used when applying Laplace's method to (4.14) to obtain

$$\frac{r_1^{-1/2}}{(1 + \kappa_1 r_1)^{1/2}} e^{-2\nu_+^\epsilon \epsilon^{-1}(r_1 - r_b)} \sim \frac{r_2^{-1/2}}{(1 + \kappa_2 r_2)^{1/2}} e^{-2\nu_+^\epsilon \epsilon^{-1}(r_2 - r_b)}. \quad (5.14)$$

Since  $r_1 = 2r_{in} - r_2$ , we conclude that

$$r_1 \sim r_{in} + \frac{\epsilon}{8\nu_+^\epsilon} \log \left( \frac{1 + \kappa_2 r_{in}}{1 + \kappa_1 r_{in}} \right), \quad r_2 \sim r_{in} - \frac{\epsilon}{8\nu_+^\epsilon} \log \left( \frac{1 + \kappa_2 r_{in}}{1 + \kappa_1 r_{in}} \right). \quad (5.15)$$

Note that when  $|\kappa_1| > |\kappa_2|$ , then  $r_1 > r_{in}$  and  $r_2 < r_{in}$ . Thus, the center of the equilibrium bubble solution is located on  $\mathcal{C}$  at an  $O(\epsilon)$  distance from  $x_{in}$  in the direction of the contact point where the magnitude of the curvature is smaller.

We now briefly consider the case when  $\mathcal{B}$  makes exactly three-point contact with the boundary of a strictly convex domain. Let  $x_{in}$  be the unique location of the center of  $\mathcal{B}$ . Then, by using Laplace's method on (4.14), it is clear that (4.14) is asymptotically satisfied when  $x_0^\epsilon = x_{in}$  provided that the curvatures at the three contact points are equal and that the angles between adjacent line segments joining  $x_{in}$  to the contact points are  $120^\circ$  apart. An example of this situation is illustrated in Fig. 11 where we show the location of the equilibrium bubble solution corresponding to the triangular shaped domain given in Fig. 6. In the more typical case when the angles are not  $120^\circ$  apart or when the curvatures at the contact points are unequal, the center  $x_0^\epsilon$  is shifted by an  $O(\epsilon)$  amount away from  $x_{in}$ . A similar analysis as was given above for the two-point contact case can be done to calculate this shift precisely. The result is as follows:

**Corollary (Three-Point Contact):** *Assume that  $\mathcal{B}$  is uniquely defined and that  $\mathcal{B}$  makes exactly three-point contact with  $\partial D$  at  $x(\xi_i) \in \partial D$  for  $i = 1, 2, 3$ . Suppose also that  $\kappa_i r_{in} > -1$  for  $i = 1, 2, 3$ , where  $\kappa_i \leq 0$  is the curvature of  $\partial D$  at  $x(\xi_i)$ . Then,  $x_0 = x_0(\epsilon)$  satisfies*

$$x_0(\epsilon) = x_{in} + \epsilon x_0^1 + O(\epsilon^2), \quad (5.16)$$

where  $x_0^1$  is the solution to the linear system

$$\begin{aligned} (\hat{n}_3 - \hat{n}_1) \cdot x_0^1 &= (2\nu_+^\epsilon)^{-1} \{ \log(A_1/A_3) + \log(-\hat{n}_1 \cdot \hat{t}_2 / \hat{n}_3 \cdot \hat{t}_2) \}, \\ (\hat{n}_1 - \hat{n}_2) \cdot x_0^1 &= (2\nu_+^\epsilon)^{-1} \{ \log(A_2/A_1) + \log(-\hat{n}_2 \cdot \hat{t}_3 / \hat{n}_1 \cdot \hat{t}_3) \}. \end{aligned} \quad (5.17)$$

Here  $A_i = (1 + \kappa_i r_{in})^{-1/2}$  and  $\hat{n}_i$  and  $\hat{t}_i$  are the unit outward normal vector and the unit tangent vector at  $x(\xi_i) \in \partial D$ , respectively. A similar result is obtained in [28] for equilibrium spike-type solutions to a class of reaction-diffusion equations in a multi-dimensional domain.

Finally, when the domain is not strictly convex the center  $x_{in}$  of  $\mathcal{B}$  may not be uniquely determined. For instance, consider the rectangular domain  $|x_1| < b_1$ ,  $|x_2| < b_2$  with  $b_1 > b_2$ . Then,  $r_{in} = b_2$  and  $x_{in}$  is any point on the line segment  $x_2 = 0$  with  $|x_1| < b_1 - b_2$ . In this degenerate case, a simple application of Laplace's method on (4.14) shows only that the bubble must lie on this line segment. However, by examining the subdominant contributions to the integral in (4.14) away from the contact points it is clear that (4.14) will be asymptotically satisfied only when  $x_0^\epsilon = (0, 0)$ .

## 6. Slow Bubble Motion in $N \geq 2$ Dimensions

We now analyze (4.13) when  $N \geq 2$ . Let  $\xi = (\xi_1, \dots, \xi_{N-1})$  be a parameterization of the  $N - 1$  dimensional surface  $\partial D$ . Suppose that at time  $t = 0$ , the distance  $r(\xi, 0) = |x(\xi) - x_0(0)|$  is minimized at a unique point  $x(\xi_0) \in \partial D$  where  $\xi = \xi_0$ . Then, as in the case  $N = 2$ , it can be shown that the motion of the center of the bubble, in the limit  $\epsilon \rightarrow 0$ , is in the direction of the vector  $x(\xi_0) - x_0(0)$  for  $t > 0$ .

To derive an explicit ODE for the distance  $r_m(t)$  between  $x(\xi_0)$  and  $x_0(t)$  we need to evaluate the following surface integral asymptotically:

$$I_{N-1} = \int_{\partial D} r^{1-N} e^{-2\nu_+^\epsilon \epsilon^{-1}(r-r_b)} [1 + \hat{r} \cdot \hat{n}] \hat{r} \cdot \hat{n} dS. \quad (6.1)$$

The dominant contribution for  $I_{N-1}$  arises from the region near  $\xi = \xi_0$ . The Hessian of  $r(\xi, t)$  at  $\xi_0$  can be diagonalized by choosing the parametrization of  $\partial D$  such that each  $\xi_j$ , for  $j = 1, \dots, N - 1$ ,

corresponds to arclength along one of the principal directions passing through  $\xi_0$ . An application of the multi-dimensional Laplace's method (see [6]) then yields

$$I_{N-1} \sim 2 \left( \frac{\pi \epsilon}{\nu_+^\epsilon r_m} \right)^{(N-1)/2} H(r_m) e^{-2\nu_+^\epsilon \epsilon^{-1}(r_m - r_b)}, \quad \text{as } \epsilon \rightarrow 0. \quad (6.2)$$

The function  $H(r_m)$  is defined to be the product of  $N - 1$  factors of the form

$$H(r_m) \equiv (1 - r_m/R_1)^{-1/2} (1 - r_m/R_2)^{-1/2} \dots (1 - r_m/R_{N-1})^{-1/2}. \quad (6.3)$$

Here  $R_j \geq 0$  for  $j = 1, \dots, N - 1$ , are the principal radii of curvature of  $\partial D$  at  $x(\xi_0)$ . In obtaining (6.2) we have assumed that the non-degeneracy condition  $R_j > r_m$  for  $j = 1, \dots, N - 1$  holds. Substituting (6.2) into (4.13) leads to the following explicit result.

**Proposition (Slow Bubble Motion  $N \geq 2$ ):** *Assume that at  $t = 0$ ,  $x(\xi_0)$  is the unique point on  $\partial D$  which is closest to  $x_0(0) = x_0^0$ . Then, for exponentially long times and for  $\epsilon \rightarrow 0$ , the motion of the center of the bubble is in the direction of  $x(\xi_0) - x_0^0$  and the distance  $r_m(t)$  satisfies the asymptotic ODE*

$$\dot{r}_m \sim -\zeta r_m \left( \frac{\epsilon}{r_m} \right)^{(N+1)/2} H(r_m) e^{-2\nu_+^\epsilon \epsilon^{-1}(r_m - r_b)}. \quad (6.4)$$

In addition,  $\mu(t)$  satisfies

$$\mu \sim -\frac{\zeta \beta}{N(s_+ - s_-)} \left( \frac{\epsilon}{r_m} \right)^{(N-1)/2} H(r_m) e^{-2\nu_+^\epsilon \epsilon^{-1}(r_m - r_b)}. \quad (6.5)$$

Here  $\zeta$  is defined by

$$\zeta = \frac{2N a_+^2 \nu_+^2}{\Omega_N \beta} \left( \frac{\pi}{\nu_+^\epsilon} \right)^{(N-1)/2}. \quad (6.6)$$

When  $N = 2$ , the results agree with those in §5.

Using Laplace's method on (3.29), we can estimate the exponentially small eigenvalues for  $\epsilon \rightarrow 0$  as

$$\lambda_j \sim \zeta \nu_+ \left( \frac{\epsilon}{r_m} \right)^{(N-1)/2} H(r_m) \left[ \hat{r}_m \cdot \hat{i}_j \right]^2 e^{-2\nu_+^\epsilon \epsilon^{-1}(r_m - r_b)}, \quad j = 1, \dots, N. \quad (6.7)$$

Here  $\hat{i}_j$  is the unit basis vector in the  $x_j^{\text{th}}$  direction.

For the ODE (6.4), suppose that  $r_m(0) = r_0 > r_b$ . The collapse time  $t_c$  is again defined by  $r_m(t_c) = r_b$ . For  $\epsilon \rightarrow 0$ , it is easy to show from (6.4) that  $t_c$  satisfies

$$t_c \sim \frac{\epsilon^{(1-N)/2}}{2\zeta \nu_+^\epsilon} f(r_0) \left[ 1 - \frac{\epsilon}{4\nu_+^\epsilon} \left( \frac{N-1}{r_0} - \sum_{i=1}^{N-1} \frac{1}{(R_i - r_0)} \right) \right] e^{2\nu_+^\epsilon \epsilon^{-1}(r_0 - r_b)}. \quad (6.8)$$

Here  $f(r_0) \equiv r_0^{(N-1)/2} [H(r_0)]^{-1}$  and  $H(s)$  is defined in (6.3).

**Example 6.1** Set  $N = 3$  and let  $D$  be an ellipsoid with boundary  $x_1^2/3^2 + x_2^2/4^2 + x_3^2/2^2 = 1$ . Suppose that the center of a bubble of radius  $r_b = .75$  is initially located at the point  $(x_1, x_2, x_3) =$

$(0, 0, 0.25)$ . Then, until the bubble collapses against  $\partial D$ , the motion of the center of the bubble is towards the closest point on  $\partial D$ , which is  $(0, 0, 2)$ . The principal radii of curvature at  $(0, 0, 2)$  are  $R_1 = 4.5$  and  $R_2 = 8.0$ . With  $r_m(0) = 1.75$  and  $Q = Q_o(u)$ , in Fig. 12 we plot the trajectories  $\log_{10}(1+t)$  versus  $r_m(t) - r_b$  for three different values of  $\epsilon$ . These trajectories were computed numerically from (6.4) using the dynamical re-scaling method of [27]. Numerical values for the parameters  $\nu_+^\epsilon$  and  $\zeta$  used in (6.4), which were calculated from (2.8), (2.14), (2.22a) and (6.6), are given in Table 5. In Table 5 we also show the favorable comparison between the asymptotic collapse time (6.8) and the corresponding numerical result computed from (6.4).

Finally, we remark that the determination of the equilibrium bubble center  $x_0^\epsilon$  proceeds as in the  $N = 2$  case considered in §5.2. Suppose that the center  $x_{in}$  of the largest sphere that can be inscribed within  $D$  is uniquely determined. Then, by using Laplace's method on (4.14) it follows that  $x_0^\epsilon$  is located at an  $O(\epsilon)$  distance away from  $x_{in}$ . For instance, consider the case of two-point contact and let  $N = 3$ . Then,  $x_0^\epsilon$  is located along the chord  $\mathcal{C}$  joining the contact points. Moreover, in analogy with (5.15), we obtain from (4.14) and (6.2) that

$$r_1 \sim r_{in} + \frac{\epsilon}{8\nu_+^\epsilon} \log \left[ \left( \frac{1 - r_{in}/R_1^{(2)}}{1 - r_{in}/R_1^{(1)}} \right) \left( \frac{1 - r_{in}/R_2^{(2)}}{1 - r_{in}/R_2^{(1)}} \right) \right], \quad r_2 = 2r_{in} - r_1. \quad (6.9)$$

Here  $R_j^{(i)}$  is the  $j^{\text{th}}$  principal radius of curvature of  $\partial D$  at the contact point  $\xi_i$  and  $r_1$  is the distance along  $\mathcal{C}$  from the contact point at  $\xi_1$  to the center  $x_0^\epsilon$  of the equilibrium bubble solution.

## 7. Discussion

Although the metastability results in §4-6 pertain only to the Allen-Cahn equation, we anticipate that a similar formal asymptotic analysis can be done to explicitly characterize the slow bubble motion for the Cahn-Hilliard equation and for the viscous Cahn-Hilliard equation, introduced in [20]. Such an analysis would complement the rigorous results of [2] and [3], which proved the existence of slow bubble motion for the Cahn-Hilliard equation.

Another topic for further investigation is to analyze the motion of the bubble once it has become attached to the boundary. Recall that the results in §4-6 are valid only until the bubble begins to collapse against  $\partial D$ . For the two-dimensional case, we now speculate on the qualitative behavior of the subsequent motion. To satisfy the Neumann boundary condition and to minimize the surface energy at a given time, the bubble interface must intersect  $\partial D$  at right angles and should be asymptotically close to the arc of a circle that encloses the required mass. The bubble should then move on a fast time scale in the direction where the magnitude of the curvature is increasing the most. This process decreases the surface energy and should continue until a local minimum of the surface energy is attained. Such a minimum presumably occurs near a region of  $\partial D$  where the magnitude of the curvature has a local maximum. If  $\partial D$  contains some segments where the curvature is constant, the bubble motion along  $\partial D$  may become stuck and an asymptotic metastability analysis may be required. It would be worthwhile to examine these issues in detail.

Finally, we remark on an interesting comparison between the eigenvalue problem (3.1) and the eigenvalue problem that is associated with the exit time behavior for a Brownian particle confined in a domain  $D$  by a potential well  $V$  (see [18]). To determine the expected time for this particle to

leave  $D$ , we must calculate for  $\epsilon \rightarrow 0$ , the principal eigenpair  $\lambda_0, \phi_0$  of the Fokker-Plank equation

$$\epsilon \Delta p + \nabla \cdot [p \nabla V] = \lambda p, \quad x \in D \subset \mathcal{R}^N; \quad p = 0, \quad x \in \partial D. \quad (7.1)$$

Assume that  $V$  has the form  $V = V[|x - x_0|]$  for some  $x_0 \in D$  and that  $V(0) = 0$  and  $V'(r) > 0$  for  $r > 0$ . By setting  $p = e^{-V/(2\epsilon)} \phi$  in (7.1), we obtain a problem very similar in form to (3.1)

$$L_\epsilon \phi \equiv \epsilon \Delta \phi + F(r; \epsilon) \phi = \lambda \phi, \quad x \in D; \quad \phi = 0, \quad x \in \partial D, \quad (7.2a)$$

$$F(r; \epsilon) = -\frac{\epsilon^{-1}}{4} [V'(r)]^2 + \frac{1}{2} \left[ V''(r) + (N-1)r^{-1}V'(r) \right], \quad r = |x - x_0|. \quad (7.2b)$$

Now since  $\tilde{\phi}_0 \equiv e^{-V/(2\epsilon)}$  satisfies  $L_\epsilon \tilde{\phi}_0 = 0$ , is of one sign, and fails to satisfy the boundary condition by only exponentially small terms, it follows that  $\phi_0 = \tilde{\phi}_0 + \phi_L$ , where  $\phi_L$  is a boundary layer function. Since  $V$  is radially symmetric about  $x_0$ , the error made in satisfying the boundary condition is maximized at that point  $x_m \in \partial D$  which is closest to  $x_0$ . A boundary layer analysis for  $\phi_0$  then leads to the estimate  $\lambda_0 = O(\epsilon^q e^{-\epsilon^{-1}V(r_m)})$  where  $r_m = |x_m - x_0|$  (see [18]). Therefore, the particle is most likely to exit  $\partial D$  at  $x_m$  and the expected time for exit is  $O(\lambda_0^{-1})$ . This estimate for  $\lambda_0$  is qualitatively similar to the estimate (6.7) that was derived for the bubble solution. Therefore, although the number of exponentially small eigenvalues for (3.1) and (7.2) differ, our conclusion that the bubble will move in the direction of the closest point on  $\partial D$  over an exponentially long time scale has a natural correspondence with similar behavior in the exit-time problem.

### Acknowledgments

I am grateful to Prof. D. Austin, Prof. J. B. Keller and Prof. R. Miura for some valuable discussions on the material in §5.2. I would also like to thank Dr. L. Reyna for his comments and Prof. N. Alikakos for sending me his preprints.

### Appendix A: Calculating the Bubble Radius

The radius  $r_b$  of the canonical bubble solution  $U_b[|x - x_0|; \epsilon]$  is determined asymptotically in terms of the mass  $M$  by  $M \sim \int_D U_b dx$ . Let  $D_+$  and  $D_-$  denote the subregions of  $D$  that are outside (i. e.  $r > r_b$ ) and inside (i. e.  $r < r_b$ ) the bubble, respectively. To asymptotically evaluate the mass constraint it is convenient to decompose it as

$$M \sim (V - V_-) S_+(\epsilon) + V_- S_-(\epsilon) + \int_{D_+} [U_b - S_+(\epsilon)] dx + \int_{D_-} [U_b - S_-(\epsilon)] dx. \quad (A.1)$$

Here  $V$  is the volume of  $D$ ,  $V_- = r_b^N \Omega_N / N$  is the volume of  $D_-$ ,  $\Omega_N$  is the surface area of the unit  $N$ -ball and  $S_\pm(\epsilon)$  is given in (2.12). Since the dominant contributions to the integrals in (A.1) arise from the region near  $r = r_b$ , the integrals can be evaluated for  $\epsilon \rightarrow 0$  using (2.20b). Substituting (2.20b) and (2.12) into (A.1), and retaining terms of order  $\epsilon$ , we obtain that

$$M \sim V s_+ + V_- (s_- - s_+) + \epsilon \left[ \sigma_1 V_- (\nu_+^{-2} - \nu_-^{-2}) - \sigma_1 \nu_+^{-2} V + \Omega_N r_b^{N-1} (\theta_- - \theta_+) \right]. \quad (A.2)$$

Here  $\sigma_1$  is defined in (2.8) and  $\theta_\pm > 0$  is defined by

$$\theta_+ = \int_0^\infty [s_+ - u_0(\rho)] d\rho, \quad \theta_- = \int_{-\infty}^0 [u_0(\rho) - s_-] d\rho, \quad (A.3)$$

where  $u_0(\rho)$  is given in (2.3). To obtain  $r_b(\epsilon)$  in terms of  $M$  we expand

$$r_b = r_b^0 + \epsilon r_b^1 + O(\epsilon^2). \quad (A.4)$$

Substituting (A.4) into (A.2) and collecting powers of  $\epsilon$ , we find that

$$r_b^0 = \left[ \left( \frac{N}{\Omega_N} \right) \left( \frac{Vs_+ - M}{s_+ - s_-} \right) \right]^{1/N}, \quad r_b^1 = -\frac{r_b^0}{(s_+ - s_-)N} \left[ \sigma_1^0 \nu_+^{-2} \left( \frac{V}{V_-^0} \right) + \gamma \right], \quad (A.5a)$$

where  $V_-^0$  and  $\gamma$  are defined by

$$V_-^0 = N^{-1} \Omega_N (r_b^0)^N, \quad \gamma = \sigma_1^0 (\nu_-^{-2} - \nu_+^{-2}) + \frac{N}{r_b^0} (\theta_+ - \theta_-). \quad (A.5b)$$

Here  $\sigma_1^0$  is given by the right side of (2.8) upon replacing  $r_b$  by  $r_b^0$ .

#### REFERENCES

- [1] N. Alikakos, P. W. Bates, G. Fusco, *Slow Motion for the Cahn-Hilliard Equation in One Space Dimension*, J. Differ. Equations 90, (1991), pp. 81-135.
- [2] N. Alikakos, G. Fusco, *Slow Dynamics for the Cahn-Hilliard Equation in Higher Spatial Dimensions, Part 1: Spectral Estimates*, Carr Reports in Mathematical Physics, University of Rome, (1993).
- [3] N. Alikakos, G. Fusco, *Slow Dynamics for the Cahn-Hilliard Equation in Higher Spatial Dimensions, Part 2: The Motion of Bubbles*, preprint, (1993).
- [4] U. Ascher, R. Christiansen, R. Russell, *Collocation Software for Boundary value ODE's*, Math. Comp. 33, (1979), pp. 659-679.
- [5] P. W. Bates, J. P. Xun, *Metastable Patterns for the Cahn-Hilliard Equation*, J. Diff. Equations 111, (1994), pp. 421-457.
- [6] N. Bleistein, *Mathematical Methods For Wave Phenomena*, Computer Science and Applied Mathematics Series, Academic Press, Orlando, (1984).
- [7] L. Bronsard, D. Hilhorst, *On the Slow Dynamics for the Cahn-Hilliard Equation in One Space Dimension*, Proc. Roy. Soc. London A, Vol. 439, (1992), pp. 669-682.
- [8] L. Bronsard, B. Stoth, *Volume Preserving Mean Curvature Flow as a Limit of a NonLocal Ginzburg Landau Equation*, Carnegie Mellon University Research Report No. 94-NA-008, (1994).
- [9] L. Bronsard, B. Wetton, *A Numerical Method for Tracking Curve Networks Moving with Curvature Motion*, to appear, (1995), J. Comp. Phys.
- [10] J. Cahn, J. Hilliard, *Free Energy of a Non-Uniform System. I. Interfacial Free Energy*, J. Chem. Phys. 28, (1958), pp. 258-267.
- [11] J. Carr, R. Pego, *Metastable Patterns in Solutions of  $u_t = \epsilon^2 u_{xx} - f(u)$* , Comm. Pure Appl. Math. 42, (1989), pp. 523-576.
- [12] C. M. Elliot, D. A. French, *Numerical Studies of the Cahn-Hilliard Equation for Phase Separation*, IMA J. Appl. Math. Vol. 38, (1987), pp. 97-128.
- [13] G. Fusco, J. Hale, *Slow Motion Manifold, Dormant Instability and Singular Perturbation*, J. Dynamics and Diff. Equations 1, (1989), pp. 75-94.

- [14] M. Gage, *On an Area-Preserving Evolution for Plane Curves*, Contemp. Math. 51, (1986), pp. 51-62.
- [15] C. Grant, *Slow Motion in One-Dimensional Cahn-Morrel Systems*, SIAM J. Math. Anal. Vol. 26 No. 1, (1995), pp. 21-34.
- [16] C. C. Hsiung, *A First Course in Differential Geometry*, Wiley Interscience Series in Pure and Applied Mathematics, New York (1981).
- [17] M. Kuwamura, S. I. Ei, M. Mimura, *Very Slow Dynamics for Some Reaction-Diffusion Systems of the Activator-Inhibitor Type*, Japan J. Indust. Appl. Math. 9, (1992), pp. 35-77.
- [18] B. J. Matkowsky, Z. Schuss, *The Exit Problem for Randomly Perturbed Dynamical Systems*, SIAM J. Appl. Math. Vol. 33 No. 2, (1977), pp. 365-382.
- [19] J. Neu, Unpublished Notes.
- [20] A. Novick-Cohen, *On the Viscous Cahn-Hilliard Equation*, in ‘Material Instabilities in Continuum Mechanics and Related Mathematical Problems’, (J. Ball ed.), Oxford Science Publications, Clarendon Press, (1988), pp. 329-342.
- [21] T. Ohta, M. Mimura, *Pattern Dynamics in Excitable Reaction-Diffusion Media*, in ‘Formation, Dynamics and Statistics of Patterns’, Vol. 1 (K. Kawasaki et al., eds.), World Scientific, (1990), pp. 55-112.
- [22] L. G. Reyna, M. J. Ward, *Metastable Internal Layer Dynamics for the Viscous Cahn-Hilliard Equation*, to appear, Methods and Applications of Analysis (1995).
- [23] L. G. Reyna, M. J. Ward, *Resolving Weak Internal Layer Interactions for the Ginzburg-Landau Equation*, European J. Appl. Math. Vol. 5, Part 4, (1994), pp. 495-523.
- [24] J. Rubinstein, P. Sternberg, *Nonlocal Reaction-Diffusion Equations and Nucleation*, IMA J. Appl. Math. Vol. 48, (1992), pp. 249-264.
- [25] J. Rubinstein, P. Sternberg, J. B. Keller, *Front Interaction and Nonhomogeneous Equilibria for Tristable Reaction-Diffusion Equations*, SIAM J. Appl. Math. Vol. 53 No. 6, (1993), pp. 1669-1685.
- [26] L. F. Shampine, M. K. Gordon, *Computer Solution of Ordinary Differential Equations, the Initial Value Problem*, W. H. Freeman publishers, San Francisco (1975).
- [27] M. J. Ward, *Metastable Patterns, Layer Collapses, and Coarsening for a One-Dimensional Ginzburg-Landau Equation*, Studies in Appl. Math. Vol. 91 No.1, (1994) pp. 51-93.
- [28] M. J. Ward, *An Asymptotic Analysis of Localized Solutions for some Reaction-Diffusion Models in Multi-Dimensional Domains*, submitted, Studies in Appl. Math 4/95 (20 pages).

$\epsilon$	$\nu_+^\epsilon$ (num.)	$\nu_+^\epsilon$ (asy.)	$\nu_+^\epsilon$ (num.)	$\nu_+^\epsilon$ (asy.)
0.025	1.8605	1.8606	1.8541	1.8545
0.075	1.8476	1.8483	1.8268	1.8299
0.125	1.8340	1.8360	1.7966	1.8053
0.151	1.8266	1.8296	1.7798	1.7925
0.175	1.8196	1.8237	1.7636	1.7807
0.199	1.8124	1.8178	1.7466	1.7689

**Table 1a:** Comparison of asymptotic and numerical values for  $\nu_+^\epsilon$  when  $r_b = 1$  and  $Q = Q_a(u)$  with  $c_0 = 1.2$ . The second and third columns are for  $N = 2$  and the fourth and fifth columns are for  $N = 3$ .

$\epsilon$	$\sigma_b(\epsilon)$ (num.)	$\sigma_b(\epsilon)$ (asy.)	$\sigma_b(\epsilon)$ (num.)	$\sigma_b(\epsilon)$ (asy.)
0.025	0.02159	0.02164	0.04313	0.04328
0.075	0.0645	0.0649	0.1283	0.1298
0.125	0.1070	0.1082	0.2119	0.2164
0.151	0.1290	0.1307	0.2546	0.2614
0.175	0.1492	0.1515	0.2935	0.3030
0.199	0.1693	0.1723	0.3319	0.3445

**Table 1b:** Comparison of asymptotic and numerical values for  $\sigma_b(\epsilon)$  when  $r_b = 1$  and  $Q = Q_a(u)$  with  $c_0 = 1.2$ . The second and third columns are for  $N = 2$  and the fourth and fifth columns are for  $N = 3$ .

$\epsilon$	$\lambda_0(\epsilon)$ (num.)	$\lambda_0(\epsilon)$ (asy.)	$\lambda_0(\epsilon)$ (num.)	$\lambda_0(\epsilon)$ (asy.)
0.025	$0.6234 \times 10^{-3}$	$0.6250 \times 10^{-3}$	$0.1247 \times 10^{-2}$	$0.1250 \times 10^{-2}$
0.075	$0.5591 \times 10^{-2}$	$0.5625 \times 10^{-2}$	0.01117	0.01125
0.125	0.01552	0.01563	0.03094	0.03125
0.151	0.02265	0.02280	0.04511	0.04560
0.175	0.03046	0.03063	0.06057	0.06125
0.199	0.03945	0.03960	0.07832	0.07920

**Table 2a:** Comparison of asymptotic and numerical values for  $\lambda_0(\epsilon)$  when  $r_b = 1$  and  $Q = Q_a(u)$  with  $c_0 = 1.2$ . The second and third columns are for  $N = 2$  and the fourth and fifth columns are for  $N = 3$ .

$\epsilon$	$\lambda_3(\epsilon)$ (num.)	$\lambda_3(\epsilon)$ (asy.)	$\lambda_4(\epsilon)$ (num.)	$\lambda_4(\epsilon)$ (asy.)
0.025	-0.0018758	-0.0018750	-0.0050020	-0.005000
0.075	-0.01694	-0.01688	-0.04516	-0.04500
0.125	-0.47351	-0.04688	-0.12620	-0.12500
0.151	-0.06941	-0.06840	-0.18487	-0.18241
0.175	-0.09368	-0.09187	-0.24925	-0.24500
0.199	-0.12179	-0.11880	-0.32351	-0.31681

**Table 2b:** Comparison of asymptotic and numerical values for  $\lambda_3(\epsilon)$  and  $\lambda_4(\epsilon)$  when  $r_b = 1$ ,  $N = 2$ , and  $Q = Q_o(u)$ .

label $i$	$x_{01}$	$x_{02}$	$r_m(0)$	$t_c$ (asy.) (5.9)	$t_c$ (num.)
1	0.5	0.5	1.92789	$0.627320 \times 10^{12}$	$0.627072 \times 10^{12}$
2	-0.5	-0.5	1.89187	$0.151560 \times 10^{12}$	$0.151096 \times 10^{12}$
3	-0.5	1.25	1.61271	$0.206595 \times 10^9$	$0.206501 \times 10^9$

**Table 3:** For the data in **Ex.5.1** we give the coordinates  $x_{01}$ ,  $x_{02}$ , and the initial distance  $r_m(0)$  for each initial condition in Fig. 6 and Fig. 7. The last two columns compare compare the asymptotic collapse time (5.9) with the corresponding numerical result.

label $i$	$x_{01}$	$x_{02}$	$r_m(0)$	$t_c$ (asy.) (5.9)	$t_c$ (num.)
1	0.4	1.4	2.12714	$0.516034 \times 10^{14}$	$0.515910 \times 10^{14}$
2	-0.5	1.6	1.93534	$0.482419 \times 10^{12}$	$0.482292 \times 10^{12}$
3	0.5	0.5	2.06601	$0.115260 \times 10^{14}$	$0.115230 \times 10^{14}$

**Table 4:** For the data in **Ex.5.2** we give the coordinates  $x_{01}$ ,  $x_{02}$ , and the initial distance  $r_m(0)$  for each initial condition in Fig. 8 and Fig. 9. The last two columns compare the asymptotic collapse time (5.9) with the corresponding numerical result.

$\epsilon$	$\nu_+^\epsilon$	$\zeta$	$t_c$ (asy.) (6.8)	$t_c$ (num.)
0.10	1.8667	9.6429	$0.544797 \times 10^{16}$	$0.544675 \times 10^{16}$
0.14	1.8133	9.9265	$0.421828 \times 10^{11}$	$0.421632 \times 10^{11}$
0.18	1.7600	10.227	$0.571291 \times 10^8$	$0.570823 \times 10^8$

**Table 5:** For the data in **Ex.6.1** we give the values of  $\nu_+^\epsilon$  and  $\zeta$  used in the numerical solution to (6.4). The last two columns compare the asymptotic collapse time (6.8) with the corresponding numerical result.

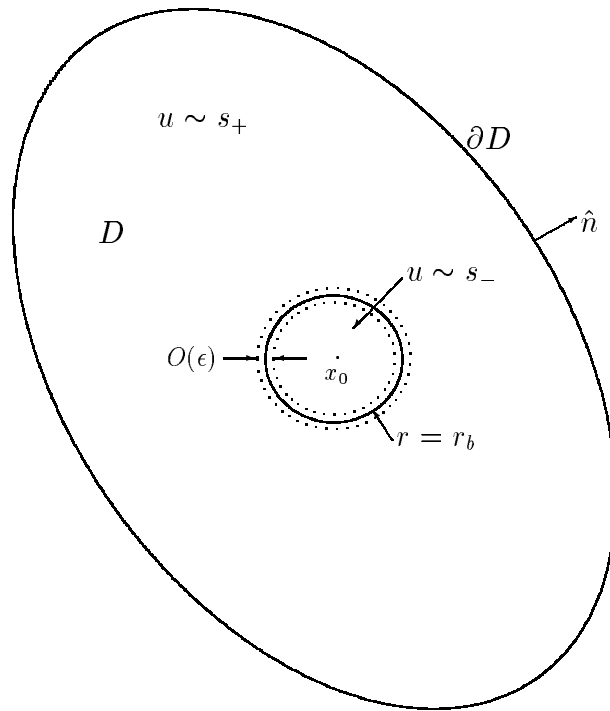


Figure 1: A bubble of radius  $r = r_b$  in a two-dimensional convex domain  $D$ .

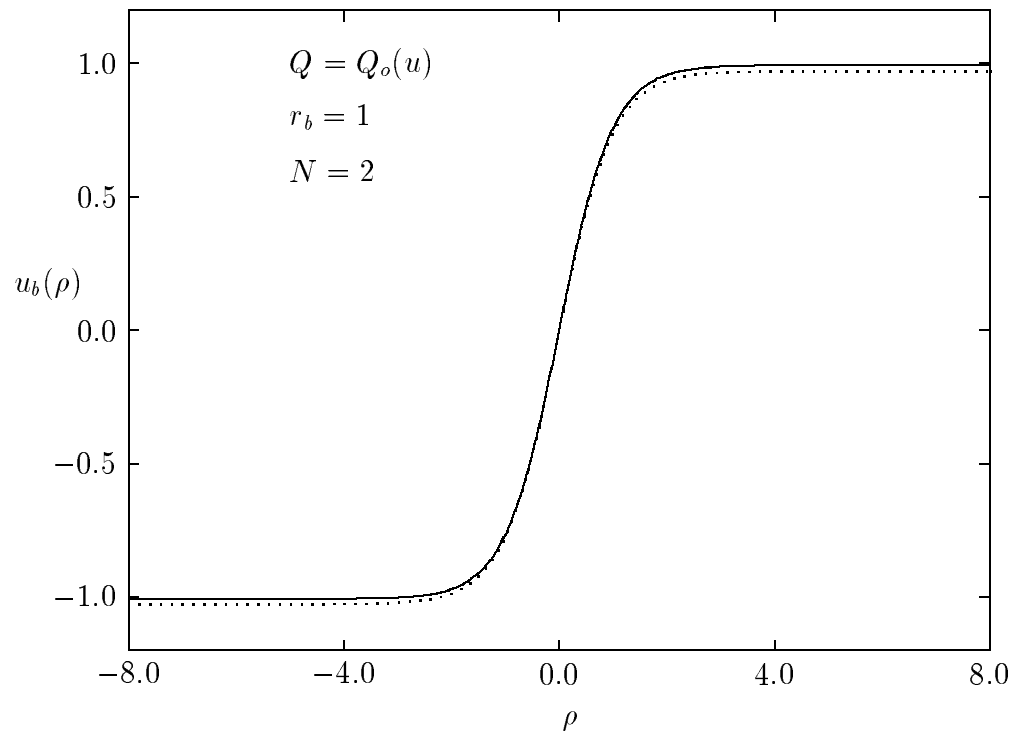


Figure 2: Plot of the computed canonical bubble solution at two different values of  $\epsilon$  when  $Q = Q_o$ ,  $r_b = 1$  and  $N = 2$ . The solid line is for  $\epsilon = .04$  and the dotted line is for  $\epsilon = .16$ .

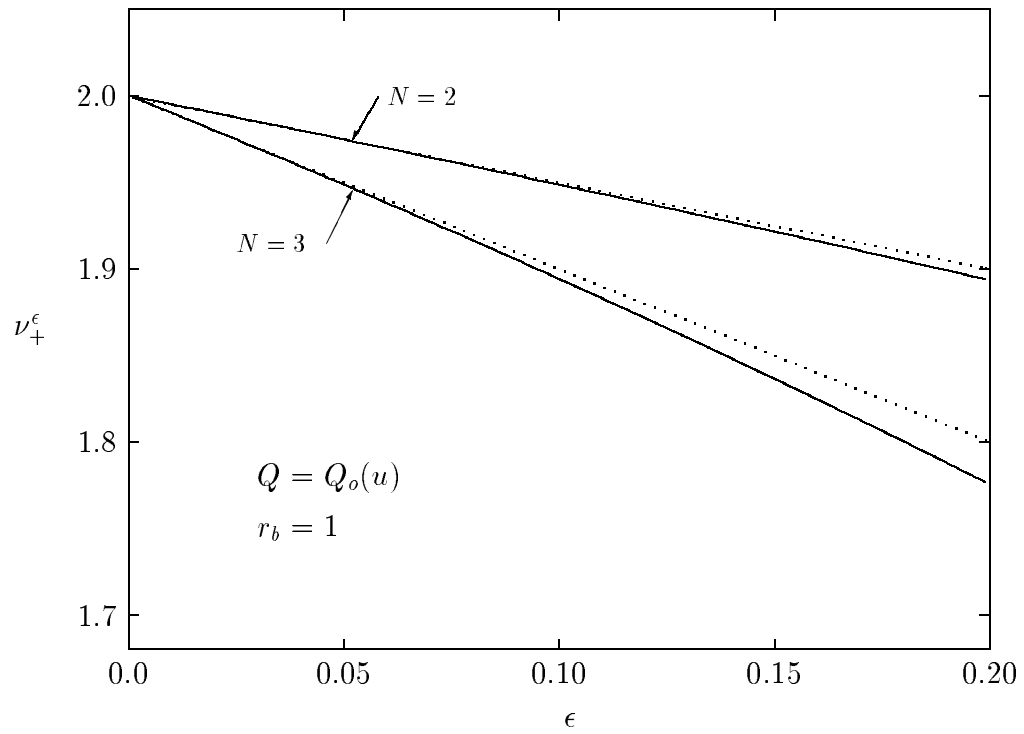


Figure 3: Comparison of asymptotic and numerical values for  $\nu_+^\epsilon$  for  $N = 2$  and  $N = 3$  when  $Q = Q_0$  and  $r_b = 1$ . The solid (dotted) lines are the numerical (asymptotic) results.

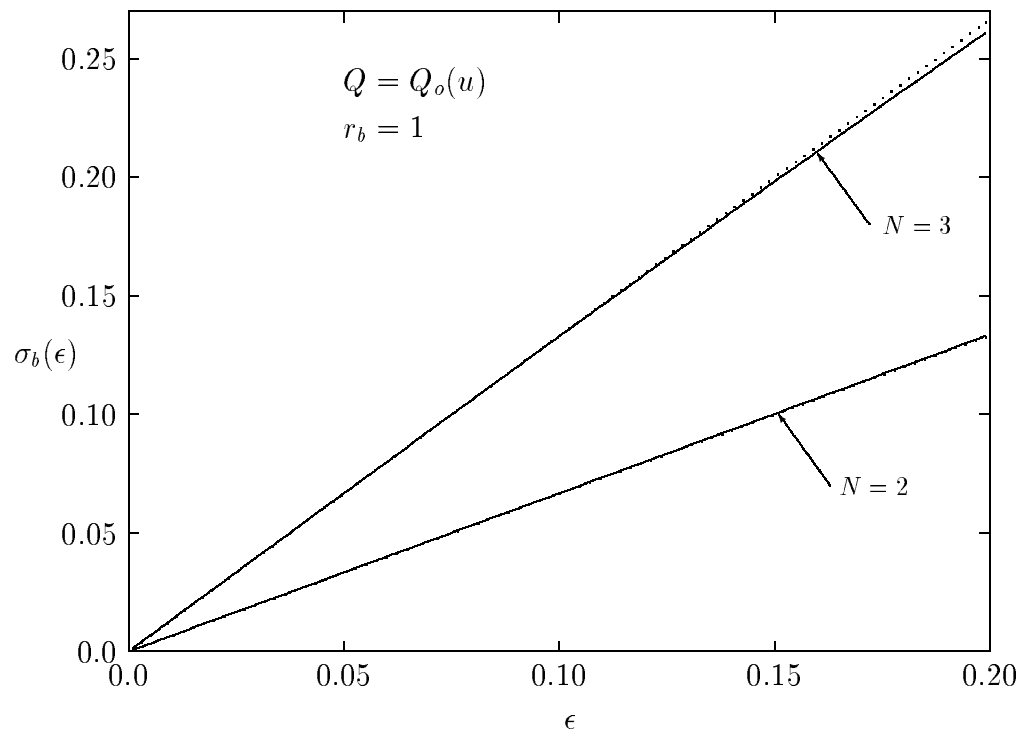


Figure 4: Comparison of asymptotic and numerical values for  $\sigma_b(\epsilon)$  for  $N = 2$  and  $N = 3$  when  $Q = Q_o$  and  $r_b = 1$ . The solid (dotted) lines are the numerical (asymptotic) results.

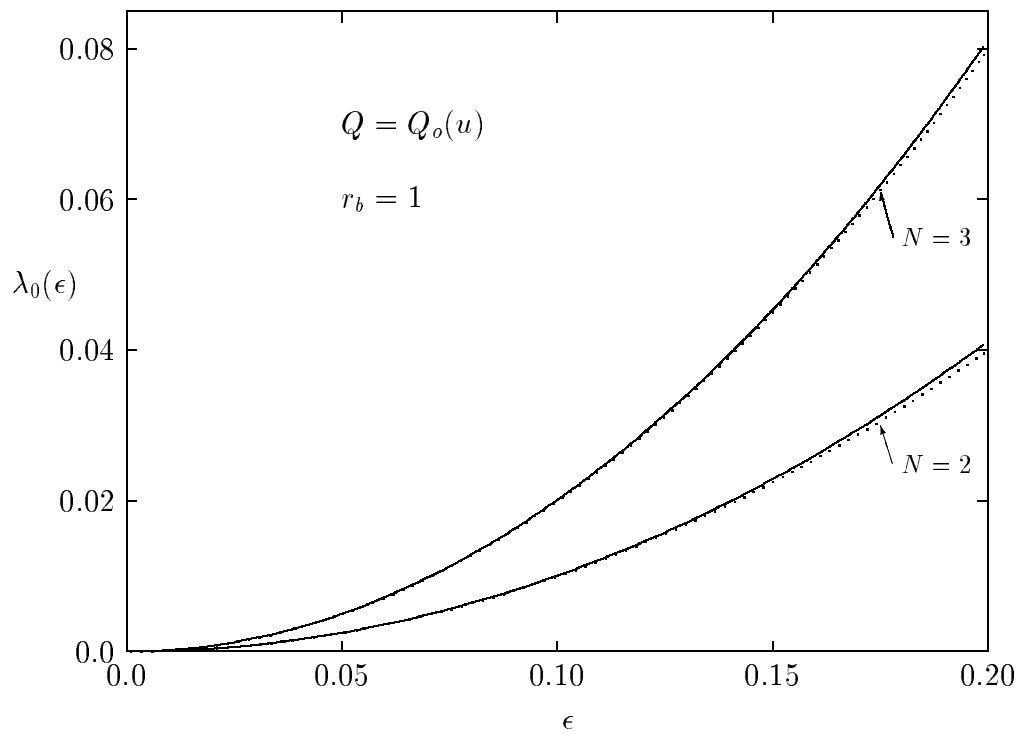


Figure 5: Comparison of asymptotic and numerical values for  $\lambda_0(\epsilon)$  for  $N = 2$  and  $N = 3$  when  $Q = Q_o$  and  $r_b = 1$ . The solid (dotted) lines are the numerical (asymptotic) results.

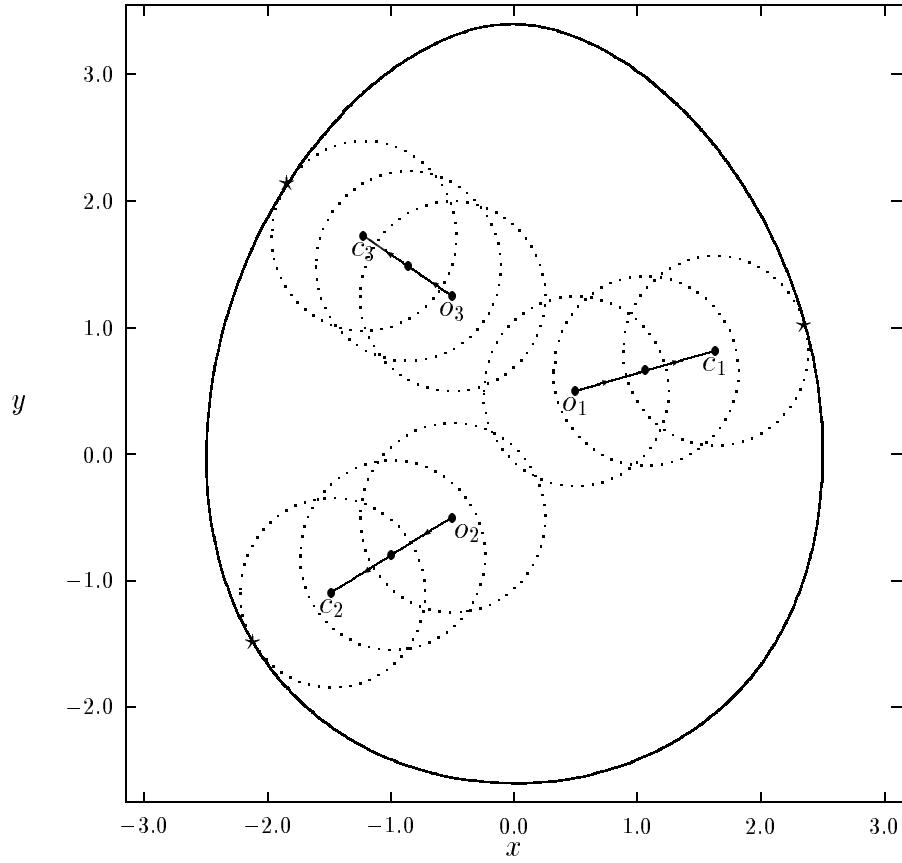


Figure 6: For  $Q = Q_o(u)$ ,  $\epsilon = .15$  and  $r_b = .75$ , we plot the motion of the center of a bubble solution for three different initial conditions. Here  $\partial D$  is parametrized by  $p(\theta) = 3 + 0.4 \sin^3(\theta) - 0.5 \cos^2(\theta)$ . The center of the bubble is initially at  $O_i$  for  $i = 1, 2, 3$ . The center then moves in the direction of the arrows until the point  $C_i$  where the bubble begins to collapse against the wall. The closest point on  $\partial D$  to  $O_i$  is labeled by  $\star$ .

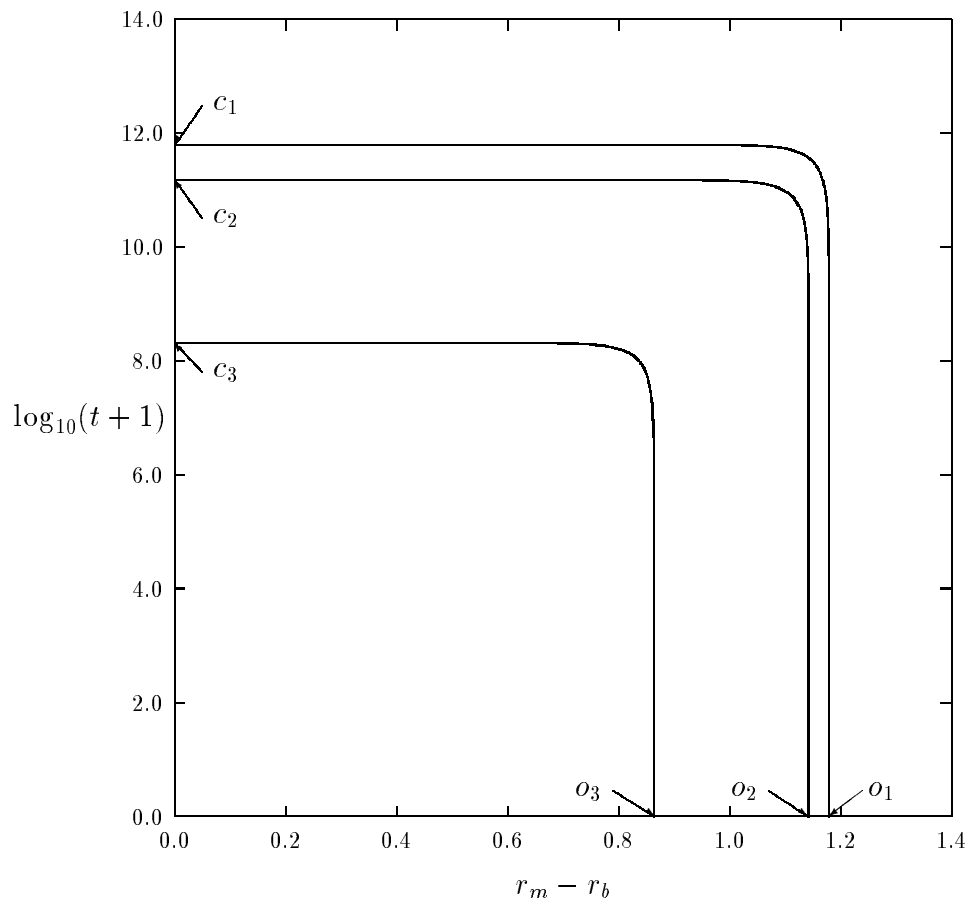


Figure 7: Plots of  $\log_{10}(1+t)$  versus  $r_m(t) - r_b$  are given for each of the trajectories shown in Fig. 6. The initial and end points for these trajectories are labeled in accordance with Fig. 6.

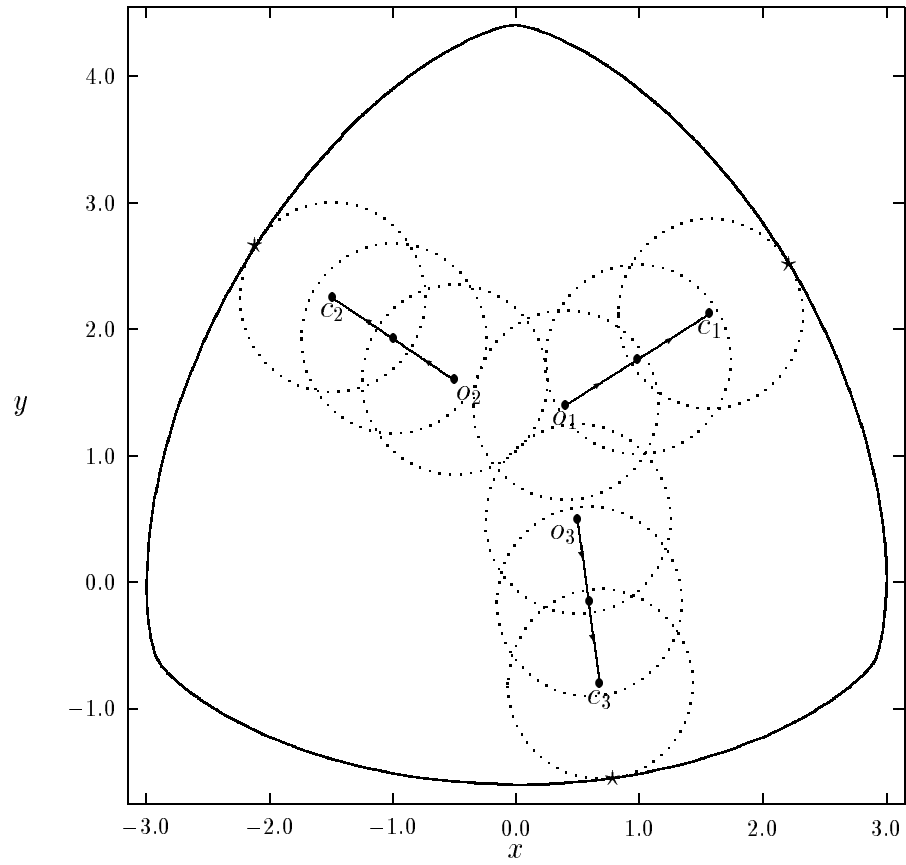


Figure 8: Same caption as for Fig. 6 except that now  $Q = Q_a(u)$ ,  $\epsilon = .15$ ,  $r_b = .75$ , and  $\partial D$  is parametrized by  $p(\theta) = 3 + 1.4 \sin^3(\theta)$ .

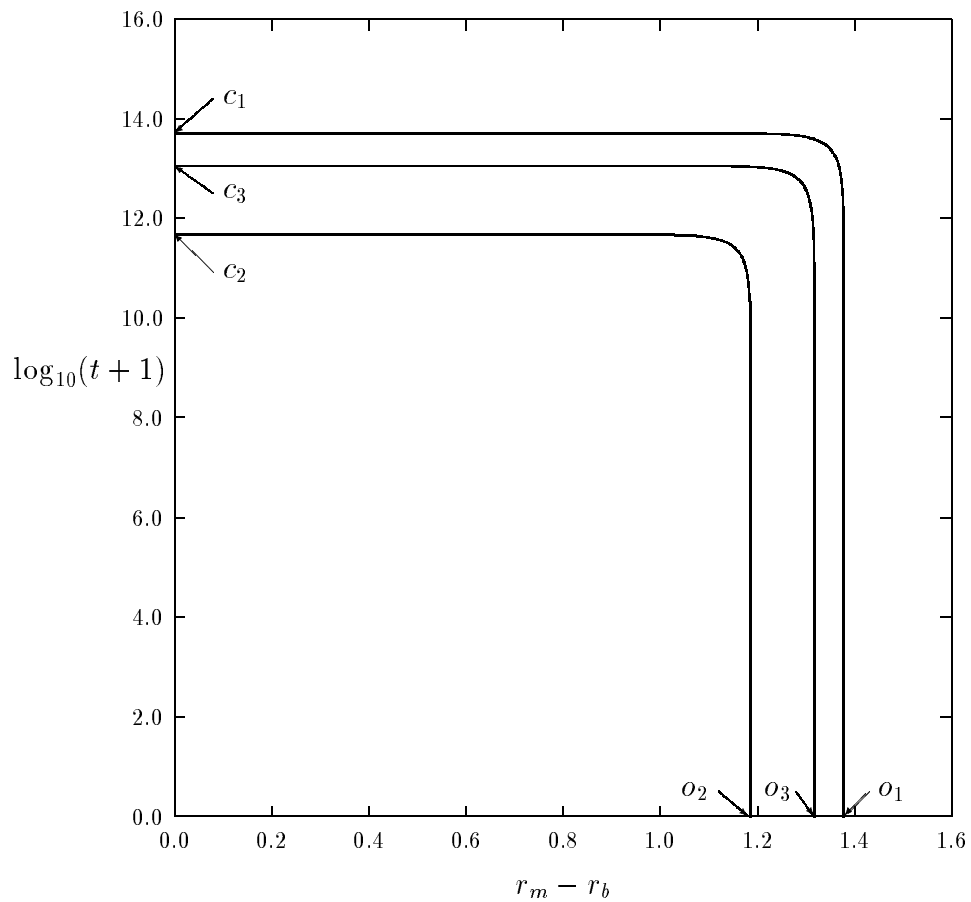


Figure 9: Plots of  $\log_{10}(1+t)$  versus  $r_m(t) - r_b$  are given for each of the trajectories shown in Fig. 8. The initial and end points for these trajectories are labeled in accordance with Fig. 8.

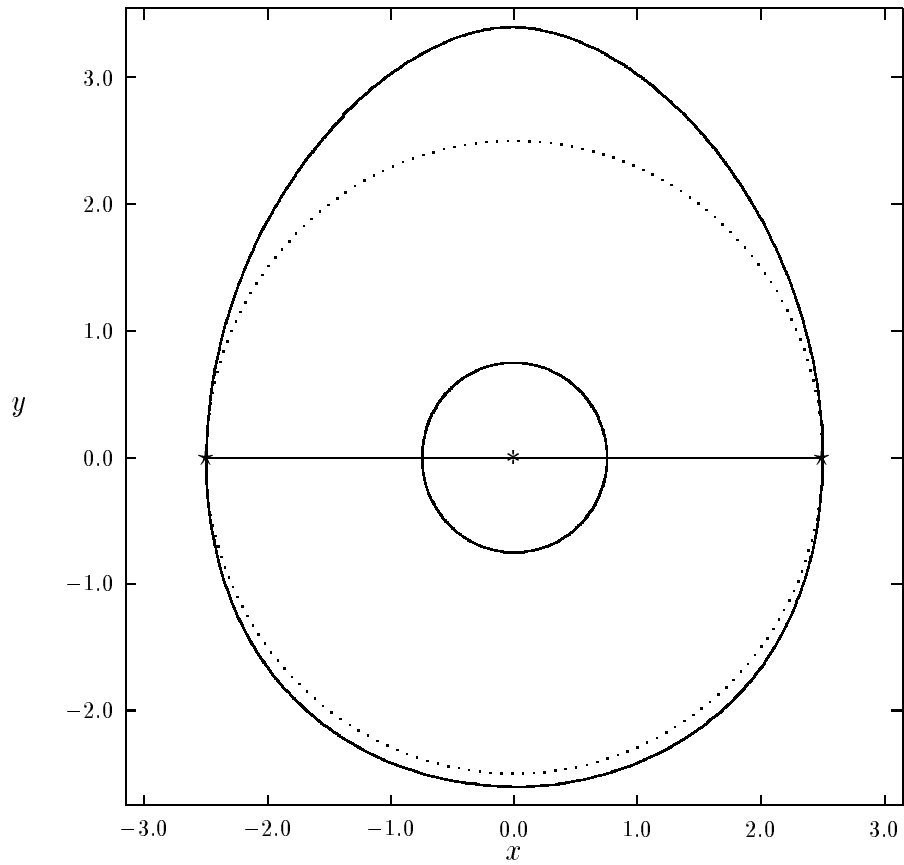


Figure 10: For the data in Fig. 6 we show the largest inscribed circle for  $D$  (labeled by the dashed circle), which is centered at the label  $*$ . The chord between the two tangent points of this circle to  $\partial D$  is shown. Since the curvature at the two tangent points is the same, the equilibrium bubble solution (labeled by the solid circle) is also centered at the point  $*$ .

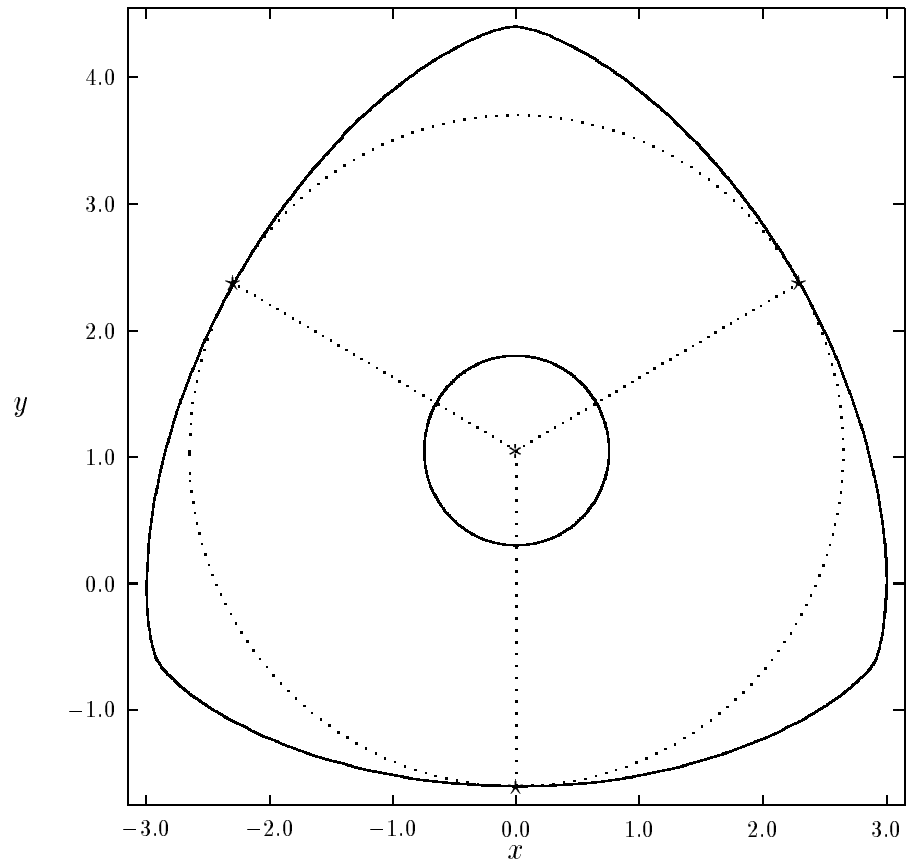


Figure 11: For the data in Fig. 8 we show the largest inscribed circle for  $D$  (labeled by the dashed circle), which is centered at the label  $*$ . The equilibrium bubble solution (labeled by the solid circle) is also centered at  $*$ .

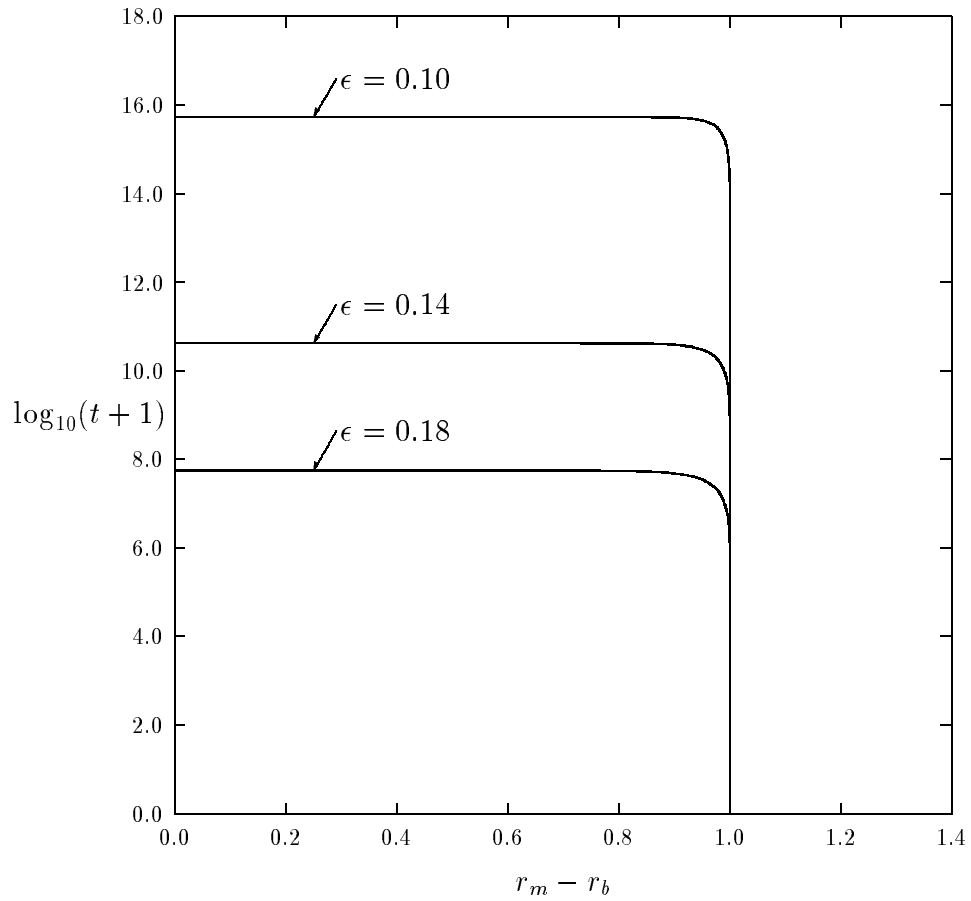


Figure 12: Plots of  $\log_{10}(1+t)$  versus  $r_m(t) - r_b$  are given for three different values of  $\epsilon$  corresponding to a bubble of radius  $r_b = 0.75$  with  $Q = Q_o(u)$  which is initially centered at the point  $(x_1, x_2, x_3) = (0, 0, 0.25)$  inside the ellipsoid  $x_1^2/3^2 + x_2^2/4^2 + x_3^2/2^2 = 1$ . The motion of the center of the bubble is towards the point  $(0, 0, 2)$  and it begins to collapse against the boundary of the ellipsoid when  $r_m = r_b$ .